

(NASA-CR-181450) REMOTE MANIPULATOR SYSTEM
(RMS)-BASED CONTROLS-STRUCTURES INTERACTION
(CSI) FLIGHT EXPERIMENT FEASIBILITY STUDY
Final Report, Oct. 1988 - Jul. 1989 (Draper
(Charles Stark) Lab.) 84 p

N90-17136

Unclas
CSCL 13I G3/37 0256761

NASA Contractor Report 181952

553957
P86

REMOTE MANIPULATOR SYSTEM (RMS) - BASED
CONTROLS - STRUCTURES INTERACTION (CSI)
FLIGHT EXPERIMENT FEASIBILITY STUDY

M. E. Demeo

The Charles Stark Draper Laboratory, Inc.
Cambridge, MA 02139

Contracts NAS9-17560 & NAS9-18147
January 1990

NASA

National Aeronautics and
Space Administration

Langley Research Center
Hampton, Virginia 23665-5225

Table Of Contents

SECTION	PAGE
1.0 Introduction.....	7
1.1 Background.....	7
1.2 Objectives of NASA's CSI Program.....	8
1.3 Why Conduct CSI Flight Experiments?.....	8
1.4 What Makes a Good CSI Experiment?.....	9
1.5 Why is RMS-Based Experiment Attractive?.....	9
1.5.1 Technology Viewpoint.....	9
1.5.2 Practical Viewpoint.....	9
1.6 Description of RMS.....	10
2.0 Overview of Experiment.....	12
2.1 Experiment Concept.....	12
2.2 Sequence of Events.....	12
2.3 Control Experiments.....	13
2.4 Big Hurdles.....	13
2.5 Cost and Schedule.....	14
3.0 Preliminary Requirements.....	15
3.1 Flexible Modes.....	15
3.2 RMS Loading (Payload).....	15
3.3 Actuators.....	16
3.4 Sensors.....	16
3.5 Experiment Computers.....	17
3.6 Carrier.....	17
3.7 Safety.....	18
3.8 RMS Life Cycle.....	18
4.0 Conceptual Design.....	20
4.1 Payload.....	20
4.1.1 SPAS Payload.....	22
4.1.2 Frequency Response of RMS/SPAS System.....	23
4.2 Actuators.....	24
4.2.1 Proof-Mass Actuators.....	24
4.2.2 Reconsideration of Payload Mounted Actuators.....	26

SECTION	PAGE
4.2.3	Use of RMS Actuators for Excitation and Control..... 26
4.3	Sensors..... 27
4.3.1	RMS Instrumentation..... 27
4.3.2	SPAS Instrumentation..... 30
4.3.3	Modal Displacement Sensors..... 30
4.3.4	Ku-Band Antenna Dither..... 30
4.4	Experiment Computer..... 32
4.4.1	Computer Speed..... 32
4.4.2	Two Fault Tolerance..... 32
4.4.3	MAST Computers..... 33
4.5	Carrier Selection..... 33
4.5.1	Hitchhiker-G Carrier..... 36
4.6	Interface Definition..... 36
4.6.1	Flexible Multiplexer Demultiplexer..... 41
4.6.2	GPC Software Modification..... 41
4.7	Safety..... 41
4.7.1	RMS Safety Strategies..... 41
4.7.2	Experiment Safety Strategies..... 43
4.7.3	Collision Avoidance..... 43
4.7.4	Dynamic Fatigue Protection..... 44
4.8	Summary of Preliminary Requirements..... 45
4.8.1	Flexible Modes..... 45
4.8.2	Payload: SPAS..... 45
4.8.3	Actuators: RMS Joint Motors..... 45
4.8.4	Sensors: Accelerometers..... 46
4.8.5	Experiment Computer: Cargo Bay Mounted Experiment Computers..... 46
4.8.6	Carrier: Hitchhiker-G..... 46
4.8.7	Interfaces..... 46
4.8.8	Safety..... 46
5.0	Test Plans..... 48
5.1	Flight Hardware and Software Integration and Testing..... 48
5.2	On-Orbit Testing..... 49

SECTION	PAGE
6.0 Schedule Estimate	50
6.1 Approach.....	50
6.2 Results.....	50
7.0 Cost Estimates	54
7.1 Approach.....	54
7.2 Results.....	54
7.3 Factors That Tend to Reduce Cost.....	54
8.0 Conclusions and Recommendations	58
9.0 Acknowledgements	59
10.0 References	60
A Acronym Definition	61
B Proof-Mass Actuator Sizing	63
C Estimate of Experiment Computer Speed	66
D Orbiter/Carrier Data Rate Estimate	68
E Growing Oscillation Mode of Failure	69
E.1 Servo Joint Control Loop.....	69
E.2 Simulation Results.....	69
F Experiment Subschedules	73
G Tasks for Phase B Definition Study	83

List Of Figures

FIGURE		PAGE
1.1	Modal Frequency Distribution vs. Controller Bandwidth.....	8
1.2	Mechanical Arm Assembly.....	11
2.1	Experiment Cartoon.....	13
4.1	Candidate Payloads.....	21
4.2	Frequency Response of RMS/SPAS System.....	25
4.3	Frequency Response of RMS/SPAS System.....	28
4.4	Experiment Computer Block Diagram.....	34
4.5	Candidate Cargo Bay Carriers.....	35
4.6	General Interface Block Diagram.....	38
4.7	Preliminary Interface Block Diagram.....	40
4.8	Performance Monitoring.....	42
6.1	Master Milestone Schedule.....	51
6.2	Phase B - Experiment Definition.....	52
6.3	Phase C/D - Preliminary Design Synthesis and Development.....	53
E.1	Control System Block Diagram.....	70
E.2	Shoulder Pitch Servo Motor Torque.....	71
E.3	Shoulder Pitch Servo Output Torque.....	72
F.1	Algorithm Design Subschedule.....	74
F.2	Modal Sensor Subschedule.....	75
F.3	Hitchhiker Subschedule.....	76
F.4	GPC Software Modification Subschedule.....	77
F.5	RMS Modification Subschedule.....	78
F.6	Experiment Computer Subschedule.....	79
F.7	Mission Operations Development Subschedule.....	80
F.8	Verification Subschedule.....	81
F.9	Second Flight Subschedule.....	82

List Of Tables

TABLE		PAGE
4.1	Payloads.....	20
4.2	SPAS Frequencies.....	23
4.3	RMS Configurations.....	23
4.4	RMS Data Acquisition Specifications.....	29
4.5	Modal Displacement Sensors.....	31
4.6	Candidate Cargo Bay Carriers.....	37
7.1	Subschedule Cost Summary.....	56
7.2	Cost Summary.....	57
E.1	RMS Load Limits.....	72

THIS PAGE
INTENTIONALLY
LEFT BLANK

Section 1 Introduction

This report documents the results of a study conducted by the Charles Stark Draper Laboratory, Inc. (CSDL) for NASA Langley Research Center (LaRC) during the period of October 1988 to July 1989.

The objective of this study was to evaluate the feasibility of conducting a Controls-Structures Interaction (CSI) experiment using the Shuttle Remote Manipulator System (RMS) with an attached payload as a test article.

1.1 Background

Presently, space vehicles and on-orbit structures are designed with the objective that the structural natural frequencies are well above the control system bandwidth (see Figure 1.1). In these cases, the lowest structural frequency is ten times greater than the controller bandwidth and it is possible to treat the structure as a rigid body. In specific application, the frequency of an isolated structural mode may lie within the bandwidth of the controller (e.g. solar panels) and in these instances, notch filtering techniques are used to lower the controller gain at the known frequency of one mode.

In contrast, future large space structures are expected to be highly flexible, due to mass minimization and large structural dimension, and to operate under the most stringent performance requirements, such as precision pointing, shape control, and vibration suppression. On account of their flexibility and performance requirements, the structural natural frequencies of these future large space systems will be nested within the control system bandwidth (see Figure 1.1). Without the separation between the control bandwidth and the lowest modal frequencies of the structure, the traditional rigid-body control methodology no longer proves adequate and the density and the unknown frequency of flexible modes make notch filtering techniques impractical. In order to avoid flexible structure and control interaction, the control system strategy must take into account the flexible body responses as well as the rigid body dynamics. The approach for accomplishing this control strategy is commonly referred to as the flexible-body control approach or the CSI approach.¹

Although there has been significant theoretical and ground test development in this field over the past fifteen years [1], there is almost a complete absence of on-orbit validation of the technology. The purpose of this study has been to investigate the feasibility of an experiment which would demonstrate the on-orbit characterization and flexible-body control of large space structure dynamics using the Shuttle RMS with an attached payload as a test article.

¹"Final Report: SSTAC AD HOC Subcommittee on Controls-Structures Interaction," 8 June 1983, pp. 3-6.

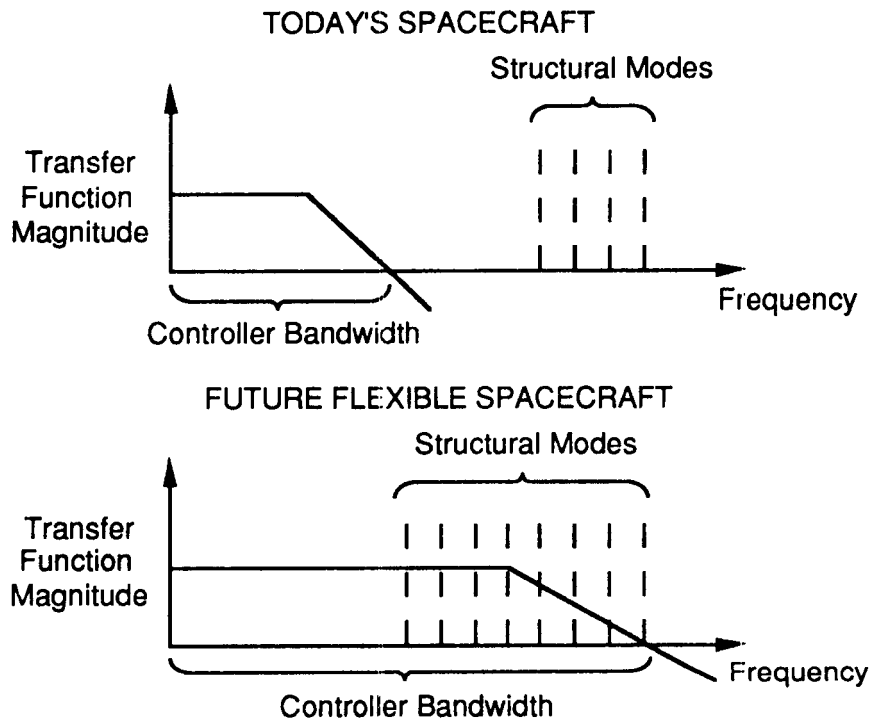


Figure 1.1: Modal Frequency Distribution vs. Controller Bandwidth

1.2 Objectives of NASA's CSI Program

NASA has recognized the need for a proven CSI technology. Towards this end they have undertaken the tasks of developing methods for the simultaneous optimization of structures and control designs, developing ground validation methods for large flexible structures and performing flight tests. These initiatives are aimed at reducing the unfavorable excitation of large space structures by 50% with a minimum increase in mass and enabling tenfold performance improvements via wider bandwidth control systems.

1.3 Why Conduct CSI Flight Experiments?

Future missions will require CSI technology. Further, the performance requirements of these future missions will dictate that many structural modes be within the bandwidth of the controller. In order to control the system dynamics, the flexible modes must be included in the system model, requiring accurate knowledge of the modal characteristics (mode shape, frequency, and damping) of the structure. Unfortunately, large flexible structures, designed for zero-g use, cannot be characterized by ground testing with sufficient accuracy to guarantee controller stability.

Thus, an in-space flight experiment is required to demonstrate that a structure can be characterized on-orbit and the modal data used to stabilize the controller and provide the required performance.

1.4 What Makes a Good CSI Experiment?

From the above discussion, it follows that a good candidate for a CSI experiment would be a structure that has closely spaced and dynamically coupled modes (as typical future missions do), that has structural modes within the bandwidth of the controller and which is difficult or impossible to accurately characterize using ground tests.

1.5 Why is RMS-Based Experiment Attractive?

1.5.1 Technology Viewpoint

The RMS is a flexible structure which can be configured to represent a typical large space structure. In addition, the structural dynamics of the RMS which include dynamically coupled and closely spaced modes are difficult to characterize using ground tests. The RMS-based experiment covers the full range of control technology from vibration suppression to multibody, large-angle maneuvers. Also, if the performance is improved, several structural modes will fall within the control system bandwidth. And finally, a successful experiment would validate analytical predictions and ground tests results.

1.5.2 Practical Viewpoint

The RMS is a flight qualified system which has well established and flight proven safety strategies. In addition, although a specially designed test structure could be better instrumented and less complicated than the RMS, an RMS-based experiment would be significantly less costly to implement. As will be discussed later, the additional hardware required for the experiment has design maturity and flight proven operational and safety strategies (e.g. the SPAS payload has a flight proven release/recapture system and a standard Hitchhiker carrier is used to support the experiment computers in the Shuttle cargo bay).

A successful experiment would not only validate CSI technology but also demonstrate an improved operational capability for both the Shuttle RMS (SRMS) and the Space Station RMS (SSRMS). Areas of potential improvement include the following:

- Improved handling of heavier payloads. As evidenced by previous missions, the dynamics of the RMS are apparent to the astronauts and become more pronounced with heavier payloads. [2]

- Improved flexible payload handling. The integrated approach of CSI technology would accommodate the dynamics of a flexible payload on the RMS.
- The authority of the on-orbit Flight Control System (FCS) can be improved by suppressing the low frequency structural dynamics of the RMS which "can feed back through the Orbiter based FCS sensors and adversely affect the FCS performance and stability". [3]
- Reduced cost of space station assembly. The experiment controller will suppress the oscillations of the RMS/payload system which add time to payload deployment, retrieval and maneuvering. On STS-8, maneuvering the 7460 lb. Payload Flight Test Article (PFTA) on the RMS it was noted that ...

Their (the oscillations) prime impact was on time, in that the crew would have to wait for the oscillations to damp sufficiently to determine the results of the last input and to insure that the next input would not be phased improperly so as to constructively enhance the oscillation. [2]

1.6 Description of RMS

The RMS is the mechanical arm of the Payload Deployment and Retrieval System (PDRS) which is responsible for the deployment, retrieval, and maneuvering of payloads. The arm is 50 ft. 3 in. in length, 15 in. in diameter, and has a mass of 905 lb.. The anthropomorphic manipulator arm is mounted on the port longeron of the Orbiter cargo bay. The RMS consists of six joints connected via structural members as shown in Figure 1.2.

From the point where the RMS is attached to the Orbiter, the arm is comprised of 2 single degree-of-freedom shoulder joints (shoulder yaw and shoulder pitch), a 21 ft. long upper boom, an elbow (pitch) joint, a 23 ft. long lower boom, 3 single degree-of-freedom wrist joints (wrist pitch, wrist yaw and wrist roll), and a snare type end effector which mates with a payload mounted grapple fixture. The structural attachment of the RMS to the Orbiter longeron is accommodated by the Manipulator Positioning Mechanism (MPM). The arm booms are made of a graphite/epoxy composite material. The joints are driven by brushless DC permanent magnet motors through low speed, high efficiency epicyclic gear trains to provide the desired torque and speed characteristics. The gear trains are designed to provide both a forward and backward drive capability. For the unloaded arm, the maximum translational rate of the end effector is 2.0 ft./sec. and the maximum rotational rate is 4.76°/sec.. The loaded arm rates vary with payload mass. With a 32k lb. payload, the maximum translational rate is 0.2 ft./sec. and the maximum rotational rate is 0.476°/sec.. [4]

The RMS was designed to deploy payloads up to 65k lb. and retrieve payloads weighing up to 32k lb.. The software that controls RMS operations resides in the Orbiter Systems Management (SM) General Purpose Computer (GPC) which sends joint angular rate commands to the individual joint servo mechanisms.

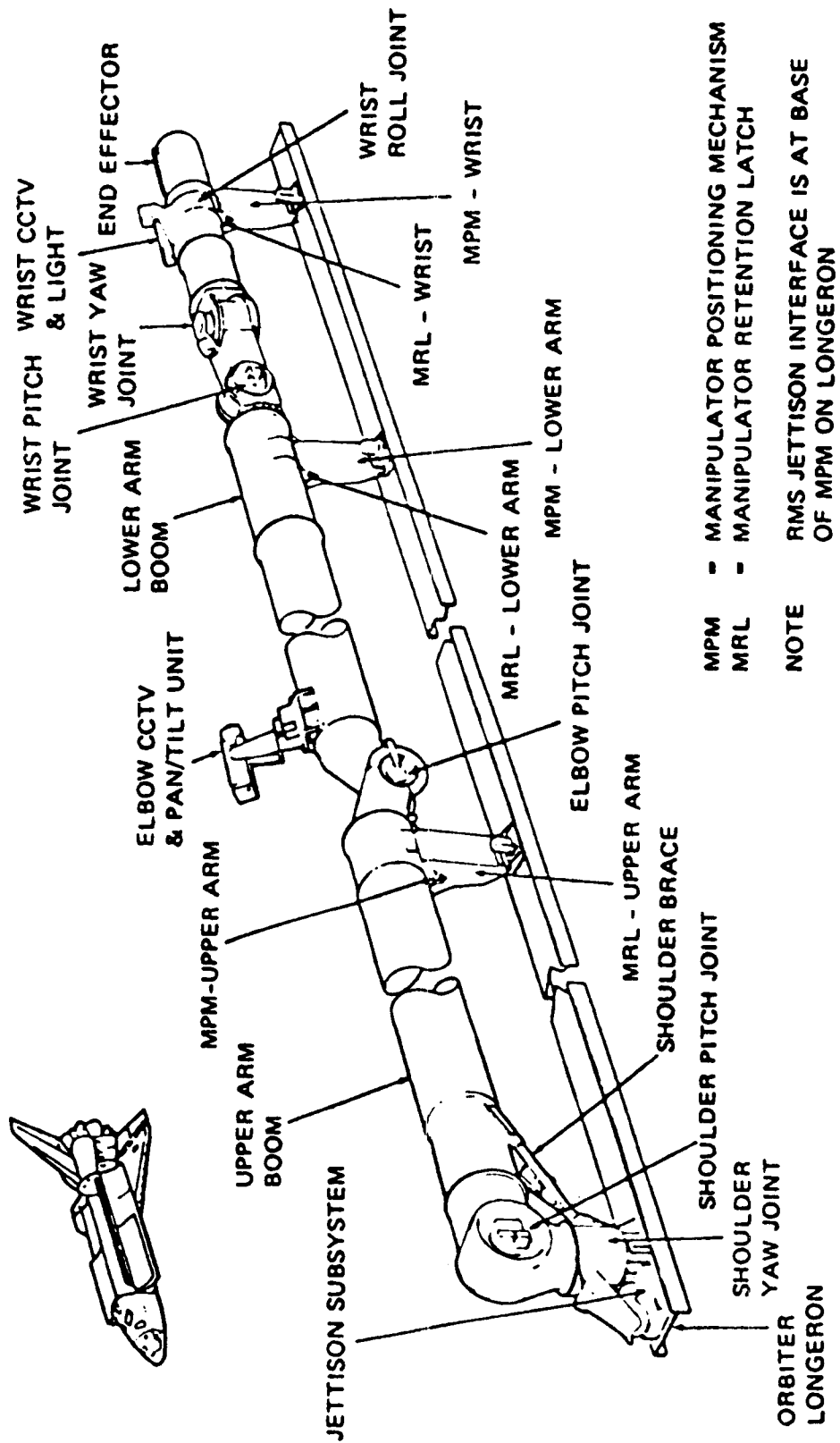


Figure 1.2: Mechanical Arm Assembly

Section 2 Overview of Experiment

The experiment definition involved a series of steps. Initial requirements were defined to the extent necessary to identify the essential trade studies. Trade studies were made to the extent necessary to define the basic elements of a viable experiment concept. A conceptual design was developed to the extent necessary to establish experiment feasibility and to allow cost and schedule estimates. Experiment requirements were then revised to reflect the conceptual design. The resulting experiment definition is overviewed in this section.

2.1 Experiment Concept

A cartoon of the experiment is shown in Figure 2.1. The figure depicts the Orbiter with the Shuttle Pallet Satellite (SPAS) payload deployed on the end of the RMS. The Hitchhiker carrier which supports the modal sensor processors and the experiment computers is also shown mounted in the cargo bay.

The SPAS is equipped with accelerometers and rate gyros and the RMS is instrumented with joint encoders and tachometers. In addition to these sensors, the use of optical sensors is depicted in order to convey the need for additional sensors to measure the modal displacement of the RMS/SPAS system. In actuality, these modal sensors will probably be accelerometers rather than optical sensors which rely on line-of-sight.

The control algorithms reside in redundant experiment computers mounted on the Hitchhiker. Control of the RMS joints is via the Orbiter General Purpose Computer (GPC).

2.2 Sequence of Events

The experiment requires two Shuttle flights. On the first flight, the RMS will be used to grapple and deploy the 4000 lb. SPAS payload into various arm configurations. The RMS/SPAS system will then be excited by use of the RMS joint servos for the purpose of system identification. The characterization data collected from the RMS, SPAS and modal sensors will be recorded and downlinked for ground processing. Between Shuttle flights, the system models will be updated and the initial control gains will be derived. On the second flight, selected characterization tests will be repeated and the data downlinked for overnight processing. The control parameters will be updated and then uplinked to the experiment computers. Vibration suppression of the RMS/SPAS system will then be executed and the performance of the control system monitored.

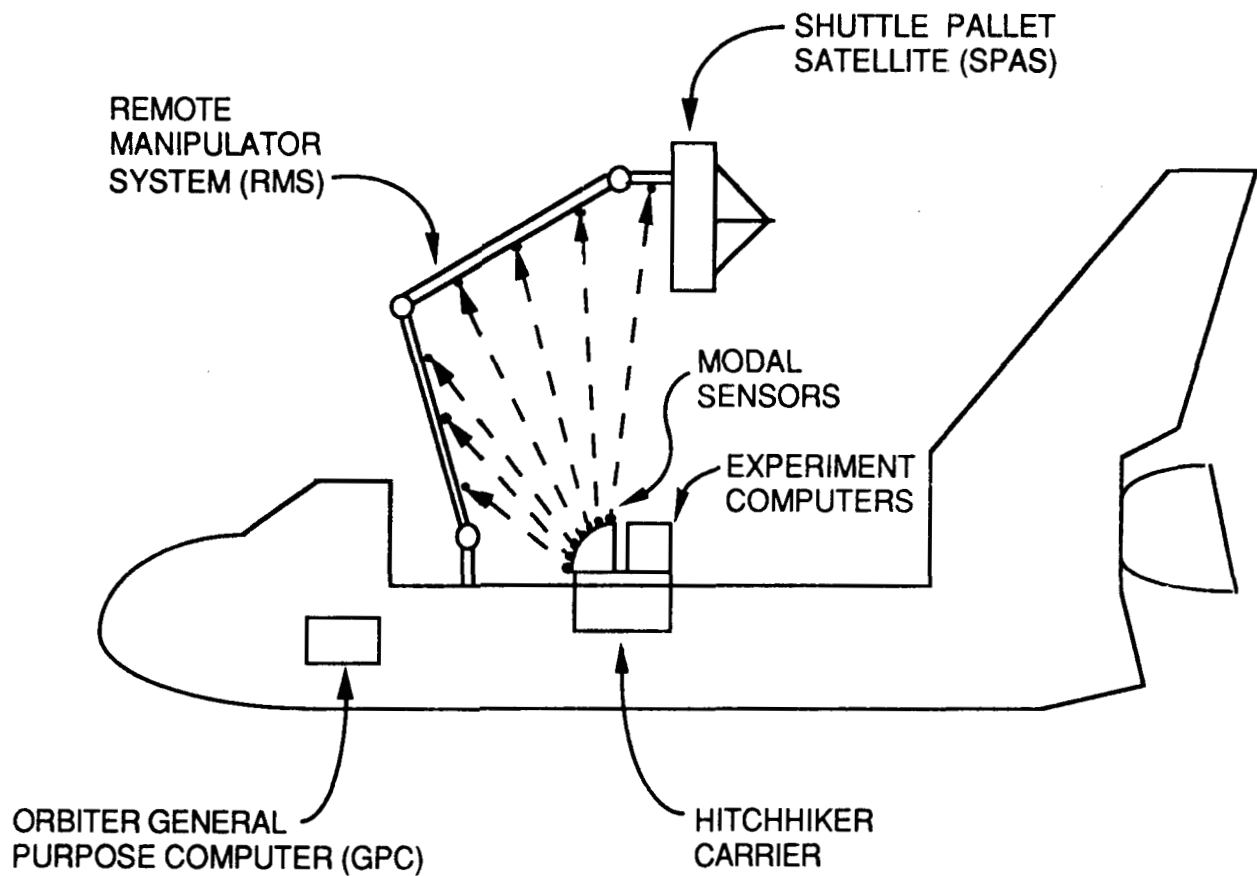


Figure 2.1: Experiment Cartoon

2.3 Control Experiments

The on-orbit experiments span the full range of difficulty of CSI problems. The experiments will be conducted in a conservative order starting with vibration suppression with a static RMS configuration (mass properties fixed) and ending with vibration suppression during large angle articulation of flexible members where variable mass properties cause continuous change in mode shape and frequency.

2.4 Big Hurdles

There are several technical and emotional hurdles which must be surmounted in order to bring this experiment to fruition. Amongst these is interfacing an experimental system with the Orbiter operational system. The experiment computer must interface with the Orbiter GPC in a

manner which is consistent with the existing safety strategies and requires minimal modification of existing GPC software. Also, the attachment of modal sensors to the flight qualified RMS must be addressed. This includes the wiring of the modal sensors and the interfacing of the modal sensor data to the experiment computers on the Hitchhiker. Additionally, the safety of the integrated experiment/operational system must be addressed. Namely, the means by which the redundant experiment computers are provided the authority to command the single-string RMS through the single-string GPC software must be established.

2.5 Cost and Schedule

Experiment cost has been minimized through the use of previously flown and/or flight qualified hardware. The RMS has a flight proven safety strategy. The SPAS payload has a flight proven release and recapture mechanism. The Hitchhiker is a standard carrier provided by GSFC. The experiment computer will be flight qualified by early 1990. Also, the required system integration and test facilities exist at the Johnson Space Center (JSC). As a result, the estimated cost of the two-flight experiment is relatively low at \$28 M. The time required for experiment development is estimated at four years.

Section 3 Preliminary Requirements

The initial requirements for the feasibility study are given below. Most of the requirements are generalized to the overall experiment objectives. The following discussion provides the rationale used to establish primary experiment requirements (P-X) and to waterfall these into secondary requirements (S-Xx).

A NASA/CSDL decision was made to use the Orbiter GPC as the interface between the experiment computer and the RMS joint servos to take advantage of the existing RMS safety strategy which is implemented in the GPC software.² With the GPC as part of the closed-loop controller, the experiment sample data rate was fixed at the GPC cycle rate of 12.5 Hz. This decision became a top-level ground rule for generating the other requirements.

3.1 Flexible Modes

P-1 At least 10 flexible modes of the experiment shall be characterized by ground-based system identification techniques applied to data taken during orbital flight. The state estimator in the on-orbit experiment shall also track 10 flexible modes. This will allow control of approximately 5 flexible modes.

S-1a The frequency of the 10th flexible mode shall be less than 1.25 Hz, to conform to standard sample data design practice.

S-1b At least one pair of closely spaced (< 10% frequency separation) and dynamically coupled (> 30% amplitude coupling) shall be obtained in at least one geometrical configuration of the RMS to provide a challenge for the controller design.

3.2 RMS Loading (Payload)

P-2 The grappled payload shall induce a sufficient inertial load on the RMS such that the first 10 flexible modes of the experiment are below 1.25 Hz. [5]

S-2a The payload should have flight proven release and recapture mechanisms to minimize experiment cost.

S-2b The payload should have sensors which allow determination of the RMS tip oscillation amplitude and the tip position.

²Demeo, Martha E., "Remote Manipulator System-Based Controls-Structures Interaction Flight Experiment Preliminary Concept Briefing at the NASA Johnson Space Center," CSDL Memo No. CSI-89-07, 11 May 1989, pp. 3-4.

- S-2c The payload should have the capability to transmit its sensor data to the Orbiter at a rate sufficient to transfer all sensor output data to the experiment computer each sample data cycle (every 0.08 seconds).
- S-2d The payload should have the capability to receive all actuator commands from the experiment computer every 0.08 seconds.
- S-2e The payload should have a power subsystem capable of supporting the payload sensors and actuators.

3.3 Actuators

- P-3 The RMS joint actuators shall be augmented by actuators located on the grappled payload, as necessary, to support the experiment's excitation and control objectives.
 - S-3a Payload actuators should be previously flight qualified to minimize cost.
 - S-3b Payload actuator bandwidth should be at least 12 Hz.
 - S-3c The actuators should be sized to be incapable of causing dynamic failure of the RMS.
 - S-3d Payload actuators should be capable of exciting the first 10 flexible modes to provide a sensed S/N > 40 dB (100:1).

3.4 Sensors

- P-4 The RMS joint encoders and tachometers shall be augmented by sensors distributed along the RMS which are capable of measuring individual boom deflections and global RMS mode shapes.
 - S-4a Modal sensors should be previously flight qualified to minimize cost.
 - S-4b Modal sensor bandwidth should be at least 12 Hz.
 - S-4c Modal sensors should not interfere with the operational capabilities of the RMS.
 - S-4d Modal sensors should be capable of providing S/N > 40 dB (100:1) at maximum

excitation amplitude of the first 10 flexible modes.

3.5 Experiment Computer

P-5 The experiment computer speed shall be sufficient for executing the excitation algorithms, state estimator algorithm, control algorithm, digital filtering, performance monitoring algorithms, and input/output functions every 0.08 seconds.

S-5a The experiment computer should be previously flight qualified to minimize experiment cost.

3.6 Carrier

P-6 A carrier shall be provided for cargo bay hardware such as the experiment computers and the modal sensor processing electronics.

S-6a The carrier shall be selected from previously flown and flight qualified carriers to minimize the experiment cost.

S-6b The carrier should be relatively small in size to minimize the cost of flying the cargo bay hardware.

S-6c The carrier shall have a data interface to the Orbiter which allows transmission of sensor data, actuator commands, estimator states, etc. from the experiment computer to the data recorders for subsequent downlink, GPC (actuator commands) and crew displays every 0.08 seconds.

S-6d The carrier shall have a command interface to the Orbiter which allows the experiment computer to receive sensor data, actuator states etc. every 0.08 seconds and also allows reloading the experiment computers from the ground uplink and crew commands which setup/start/stop the experiment.

S-6e The carrier should have a power subsystem capable of supporting the cargo bay hardware.

3.7 Safety

- P-7a The experiment shall not introduce the potential for any CRIT 1 (loss of or injury to crew or loss of Orbiter) or CRIT 2 (minor injury to crew or loss of mission) failures.
- P-7b The experiment safety strategy shall make maximum use of existing and flight proven safety algorithms, techniques, and procedures.
- S-7a Absence of dynamic interaction between an active Orbiter DAP and dormant experiment hardware shall be established by Volume XIV's Generic DAP Stability Envelope and previous on-orbit deployment of SPAS by RMS.
- S-7b Orbiter shall be in free drift mode during test period when the experiment hardware is active to eliminate the possibility of interaction of the two control systems (DAP and experiment).
- S-7c Experiment configurations shall be limited to those positions and rate boundaries and envelopes validated by previous missions to insure safe dynamic loads.
- S-7d The crew shall visually monitor the RMS motion during all test periods and the crew shall be able to manually shut down the experiment and apply RMS brakes at any instant.
- S-7e Existing safety algorithms in the SM GPC shall be retained and used.
- S-7f Experiment hardware and software shall be two fault tolerant.
- S-7g Performance monitoring algorithms shall be executed by redundant experiment computers to detect violation of performance limits.
- S-7h Performance limits shall be set well inside safety limits.
- S-7i Performance monitoring software in the redundant experiment computers shall be developed by independent parties.

3.8 RMS Life Cycle

- P-8a The experiment shall not diminish the structural integrity of or shorten the design life of the

RMS.

S-8a Performance monitoring algorithms shall detect anomalous RMS fatigue.

Section 4 Conceptual Design

This section addresses the general requirements of section 3. In the interest of readability, the details of trade studies are confined to the appendices. The preliminary requirements are summarized at the end of this section.

4.1 Payload

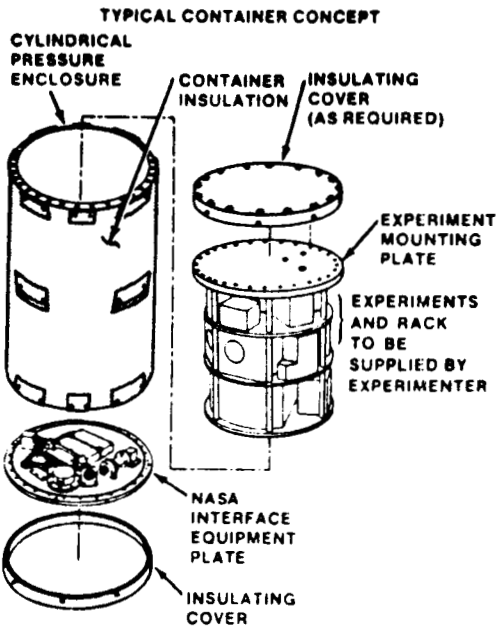
The candidates considered to provide an adequate inertial load on the RMS and to produce RMS/payload system frequencies on the order of 0.1 Hz were the (1) Get Away Special Canister (GAS CAN), (2) SPARTAN, (3) EUROpean RETrievable CARRIER (EURECA), and (4) Shuttle Pallet Satellite (SPAS). The characteristics of these payloads are summarized in the following table:

Payload	Description	Mass (lb.)			Data Management (kbps)	
		Max. User	Payload Struc.	Gross		
GAS CAN	Self-contained canister	200.	200.	400.	None	
SPARTAN	Short duration free-flyer	5,000.	1,400.	6,400.	None after unberthed	
EURECA	Reusable platform satellite	2,200.	6,600.	8,800.	Low Speed 2.	High Speed 256.
SPAS	Reusable platform satellite	1,900.	2,100.	4,000.	Command 5.	Telemetry 8.

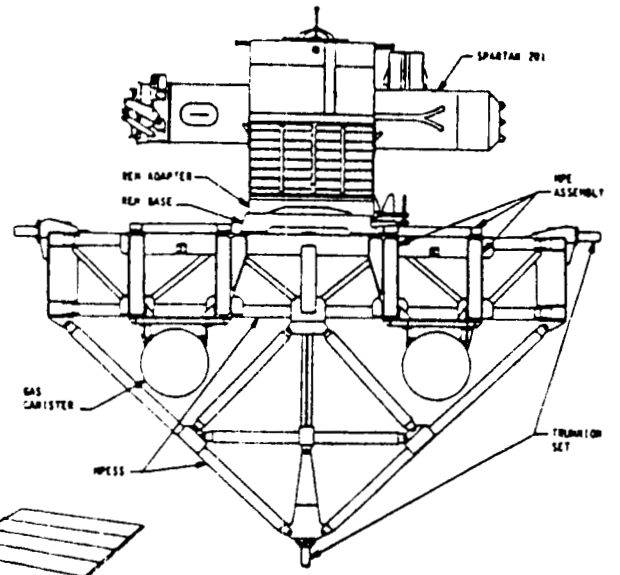
Table 4.1: Payloads

The GAS CAN is a small cylindrical self-contained payload which mounts on the side of the cargo bay (see Figure 4.1a). Although the simplicity of the GAS CAN is attractive, the mass of GAS CAN is too small to exert an adequate working load on the RMS and it is not customarily deployed with the RMS. Further, it does not provide any power, cooling or data handling capabilities. For these reasons, the choice of the GAS CAN was quickly eliminated.

The SPARTAN payload is supported in the Shuttle cargo bay by the SPARTAN Flight Support Structure (SFSS) which is a modified version of the Multi-Purpose Experiment Support Structure (MPRESS). The SFSS accommodates the SPARTAN payload with an attached Release



a. GAS CAN



b. SPARTAN

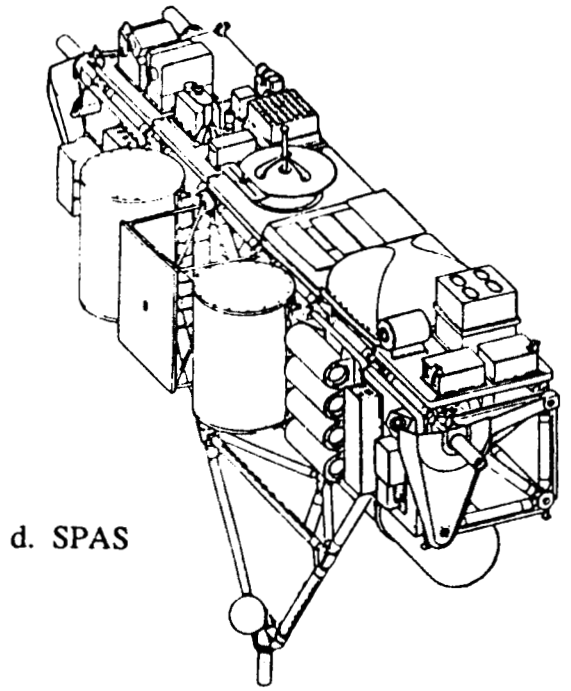
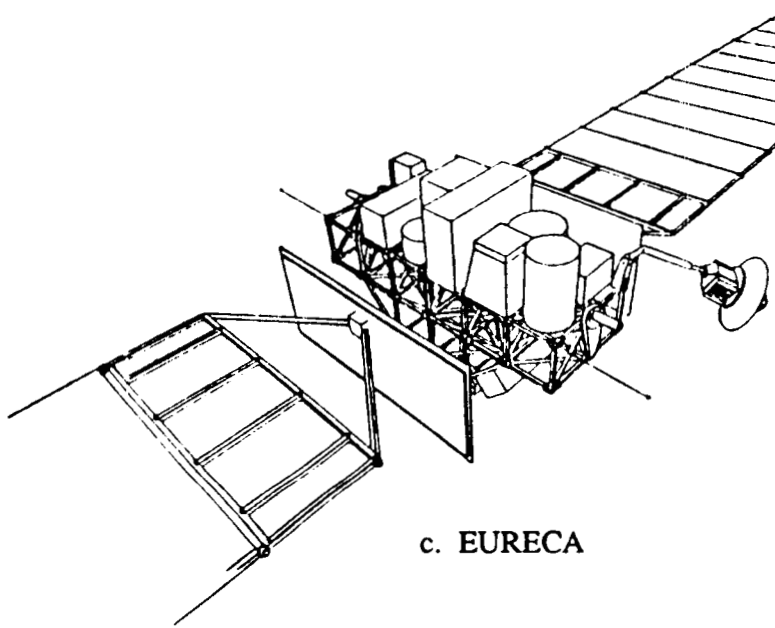


Figure 4.1: Candidate Payloads

Mechanism Base (REM) Adapter, the REM Base and two GAS CANs. It also provides the mechanical and electrical interface with the Orbiter. The gross weight of the integrated SPARTAN payload is 6400 lbs. The SFSS with SPARTAN 201 Experiment is shown in Figure 4.1b. The SPARTAN payload is fitted with a grapple fixture for RMS deployment. The SPARTAN was built by Attached Shuttle Payloads Project (Goddard Space Flight Center (GSFC)).

As shown in Figure 4.1c, the EURECA is basically rectangular in shape with some edges cut off to fit efficiently into the cargo bay. The EURECA is designed to be deployed and retrieved with the RMS and may be configured as a long duration (6-9 months) free-flyer and left in orbit for months or years before recovery by a subsequent Shuttle flight.

The SPAS is a reusable platform satellite which may be configured as a short duration (45 hours) free-flyer. The truss structure bridges the Orbiter cargo bay and interfaces with two longeron trunnions and one keel fitting. The 4k lb. SPAS was designed to accommodate grappling, deployment and recapture via the RMS. The SPAS was developed by Messerschmitt-Bölkow-Blohm (MBB) in West Germany.

4.1.1 SPAS Payload

The payload selected to meet the objectives of the RMS-Based CSI Flight Experiment was the SPAS payload. The mass of the SPAS, 4k lb., exerts a suitable inertial load on the RMS. Another attractive feature is that the SPAS's attitude control system package contains linear accelerometers and rate gyros which could be used to sense tip oscillations of the RMS/SPAS system. In addition, the SPAS has suitable communication interfaces while stowed (via hard wire umbilical) and while deployed on the RMS (via RF link). The SPAS also possesses internal power and on-board data storage capabilities. Furthermore, the SPAS is flight qualified (STS-7 and STS-11). The Strategic Defense Initiative Office (SDIO) owns SPAS³ and has agreed to the concept of time sharing with NASA on a future flight.⁴

The structural frequencies of the 3,986 lb. SPAS-01 payload are listed in Table 4.2.⁵ These structural frequencies are higher than the dominating modal characteristics of the unloaded RMS. Flight strain gauge data for the unloaded arm indicate that the modal characteristics of the arm are dominated by a mode on the order of 0.4 Hz. [6] Thus, it is anticipated that the SPAS payload may be treated as a rigid body with respect to the RMS.

³This is the SPAS-02 upon which will fly the Infrared Background Signature Survey (IBSS) payload. SDIO procured the original SPAS-01 from MBB (previously it had been leased) and have reconfigured it to meet their stringent pointing and tracking requirements.

⁴Demeo, Martha, E., "RMS/CSI Flight Experiment Technical Interchange Meeting," CSDL Memo No. CSI-89-06, 4 April 1989, p. 3.

⁵"SPAS-01: The First Shuttle Pallet Satellite Mission," Project/System Overview, Initial PIP Review at JSC, Houston, 20-22 March 1979, MBB Space Division, SPAS-01 Project Office, RX12, p. 22.

Mode	Eigenfrequency (Hz)
1	9.5
2	10.8
3	13.3
4	16.0
5	23.8
6	26.0

Table 4.2: SPAS Frequencies

4.1.2 Frequency Response of RMS/SPAS System

In order to verify that the RMS/SPAS system met the constraint imposed by the GPC cycle rate, the DRS was employed to obtain predictions of the number and frequency location of modes which may be excited by an RMS maneuver or the Orbiter Primary Reaction Control System (PRCS) jets.

The DRS was initialized with the arm in 4 different configurations which are defined by the RMS joint angles given in Table 4.3.

JOINT	JOINT ANGLES			
	B	J	WP	WPEP
SHOULDER YAW	-90.0	-82.6	0.0	0.0
SHOULDER PITCH	90.0	94.0	90.0	90.0
ELBOW PITCH	-10.0	-72.7	-10.0	-90.0
WRIST PITCH	0.0	-41.0	90.0	90.0
WRIST YAW	0.0	-7.0	0.0	0.0
WRIST ROLL	0.0	197.5	0.0	0.0

Table 4.3 RMS Configurations

The RMS/SPAS system was excited by (1) a 2.2 second command to the wrist pitch (WRP) joint followed by the application of brakes, (2) a 2.2 second command to the shoulder pitch (SHP) joint followed by the application of brakes (3) a 0.240 second duration +Pitch firing of the RCS jets with the RMS brakes on (4) a 0.44 second duration +Roll firing of the RCS jets with the RMS

brakes on and (5) a Roll Doublet consisting of a 0.64 second +Roll firing of RCS jets, a 0.08 second pulse separation and 0.64 second Roll firing of the RCS jets. The simulations were analyzed for frequency content using the Fast Fourier Transform (FFT) with a minimum 3-term Blackman Harris window. The FFT was performed on the largest resulting payload deflection (in Orbiter Body Axis Coordinates (OBAS)), i.e. XPOR, YPOR or ZPOR. The Point of Resolution (POR) defines a reference location on the payload by which the payload is positioned and about which rotations are made.

The dominance of the first bending mode of the RMS/SPAS was demonstrated in all cases and was consistently on the order of 0.1 Hz. By way of example, consider the frequency response depicted in Figure 4.2. In this case, the RMS in configuration J was excited by a +SHP maneuver. The resulting y-axis payload deflection was analyzed for frequency content using the FFT technique. The response is dominated by the mode at 0.11 Hz. The plot also depicts several modes within the 1.25 Hz constraint imposed by the GPC cycle rate.

4.2 Actuators

The original actuator options considered were to use the RMS joint motors and/or to employ SPAS mounted actuators. The candidate payload mounted actuators included Proof-Mass Actuators (PMAs), proportional thrusters and Control Moment Gyros (CMGs).

4.2.1 Proof-Mass Actuators

PMAs move a mass (the proof-mass) and use the reaction force to perform the desired work. Characteristic of this reaction principle of operation, a trade-off exists between the size of the mass and length of the stroke; i.e. big mass, small stroke. In addition, nonlinearities inherent in the design of some PMAs are difficult to overcome at lower frequencies and thereby limit the frequency range of operation of PMAs. [7]

An estimation of the size PMA which would be required, in terms of mass and stroke, to support the RMS-Based CSI Flight Experiment disclosed that for an effective RMS/SPAS mass of 5000 lbs. and a frequency of 0.1 Hz, the mass and stroke requirements to deflect the RMS/SPAS system 6 in. would be on the order of 100 lbs. and 2.7 ft., respectively (refer to Appendix B: Proof-Mass Actuator Sizing). This PMA is impractical. It is not an off-the-shelf item and development of a PMA to meet the requirements would be a formidable task. It is also too large and heavy to be a practical actuator for realistic applications. Further, a PMA of this size may be capable of causing dynamic failure of the RMS.

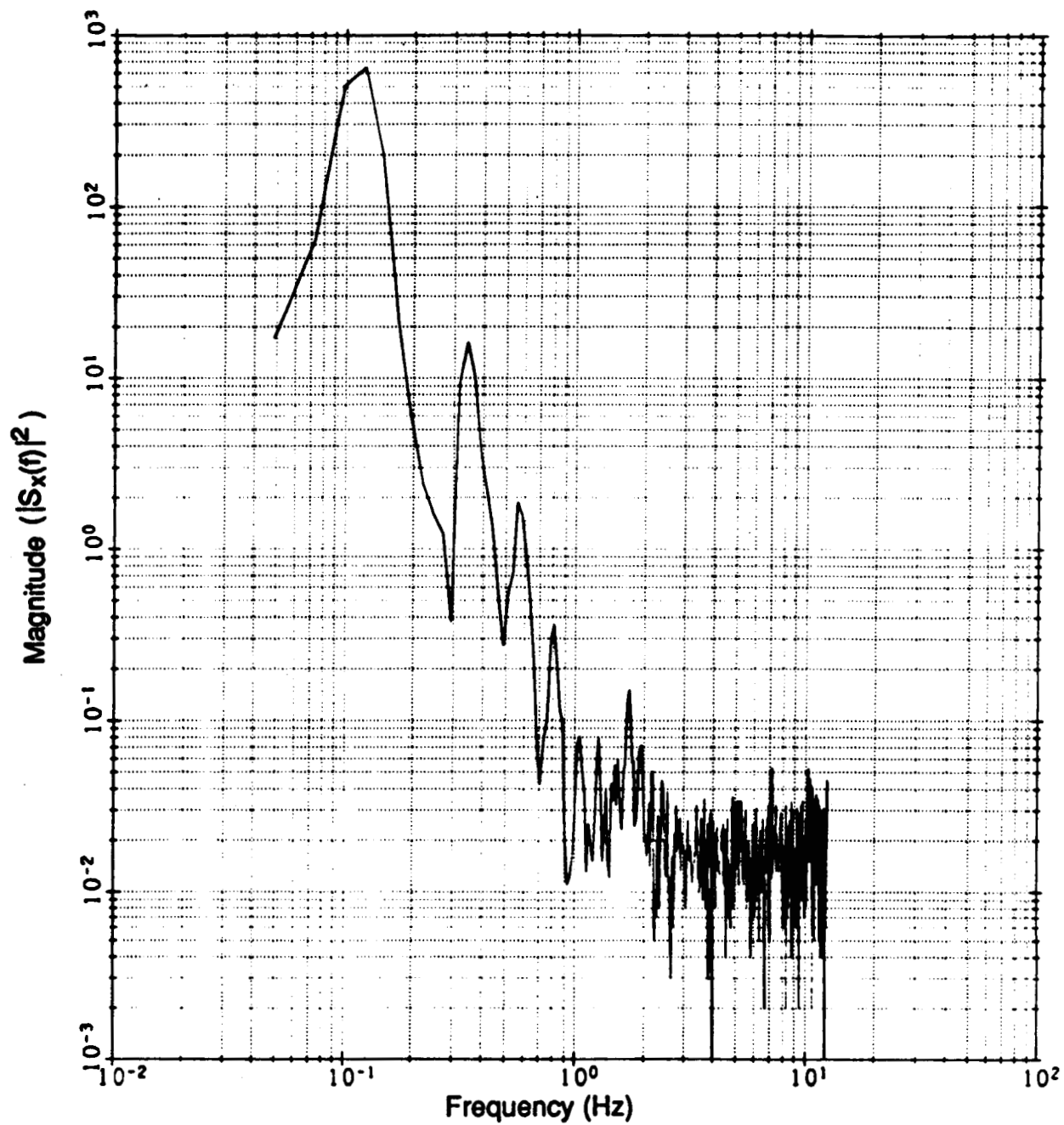


Figure 4.2 Frequency Response of RMS/SPAS System

4.2.2 Reconsideration of Payload Mounted Actuators

The original concept for the RMS-Based CSI Flight Experiment considered SPAS mounted actuators. The reasons for this were to provide excitation for dynamic characterization of the RMS, to provide actuators external to RMS for use in simple control experiments and to provide an additional control point for flexible body control experiments. The simple control experiment would use a single control point located at the tip of the RMS. However, from a technology standpoint, the simple experiment is not very attractive since a limited number of modes are controllable from a single location (possibly only one mode) and for certain geometric configurations of the RMS these controllable modes might not include the most troublesome mode. In addition, from an operational standpoint, JSC would probably have little interest in using a live load to improve RMS performance.

If payload mounted actuators were not employed, the cost of developing proof-mass actuators, modifying (and possibly flight qualifying) proportional thrusters or modifying CMG designs would be avoided and the cost of modifying the SPAS to accommodate the actuators (mechanical mounting and integration) would be avoided. In addition, safety analyses would be less extensive since it would not be necessary to prove that failures in the actuator control loops could not overload or dynamically fail the RMS structure. Thus, it became apparent that technical risk and cost could be minimized if the SPAS actuators could be eliminated. Therefore, it was decided midstream to discontinue the SPAS actuator analysis and to investigate the feasibility of using the RMS joint motors for excitation and control. If the RMS joint motors were adequate, the SPAS actuators would be eliminated.

4.2.3 Use of RMS Actuators for Excitation and Control

Based upon the desire to eliminate the option of SPAS mounted actuators, the feasibility of using the RMS joint motors for excitation and control was investigated.

As is evidenced in the DRS/FFT analysis described in section 4.1 and in the mission histories, actuation of the RMS joint motors can perturb the RMS/payload system. In addition, given the objectives of the RMS-based CSI experiment to control at least 5 modes (2 in-plane, 2 cross-axis and 1 torsional) for each arm configuration, an effort was undertaken to determine if the higher modes (i.e. modes higher in frequency than the dominant first mode) may be selectively excited by the RMS joint maneuvers. The ability to selectively excite the higher modes of the RMS/SPAS system would be particularly useful for system identification.

Higher mode excitation of the RMS/SPAS system was demonstrated using the DRS with the RMS/SPAS system initialized in configuration J (refer to Table 4.3). The RMS was driven with a sinusoidal rate command to the Wrist Yaw (WRY) joint using a modified version of the DRS,

Fixed Point (FXPT). The driving frequency of this sinusoid, $f = 0.4$ Hz, was selected from the previous simulation of a nominal +WRY command to the RMS/SPAS system in the same configuration. The amplitude of the sinusoid servo rate command was selected to produce WRY joint rates below the limit specified by the Level-C⁶ data for the SPAS payload (< 0.6 °/sec).⁷ The FFT analysis was once again performed on the largest resulting payload deflection. The frequency response of the x-axis deflection of previous +WRY maneuver is shown in Figure 4.3 (a) and the x-axis deflection response for the sinusoidal excitation of the WRY joint is given in Figure 4.3 (b). The latter plot depicts the selective excitation of the 0.4 Hz mode. The 0.4 Hz mode is raised approximately 15 dB while the magnitude of the first mode at 0.13 Hz is lowered nearly 30 dB.

4.3 Sensors

The high fidelity system identification required for the CSI problem will exceed the capability of existing RMS and SPAS instrumentation. This instrumentation was primarily intended to support the systems' operational capabilities. The specific sensors and actuators were not chosen or located on the arm or payload for the purposes of facilitating system identification. [5] As a result, these sensors shall be supplemented by modal displacement sensors distributed along the RMS. Before discussing the modal sensor candidates, the following overviews of the RMS and SPAS instrumentation are presented.

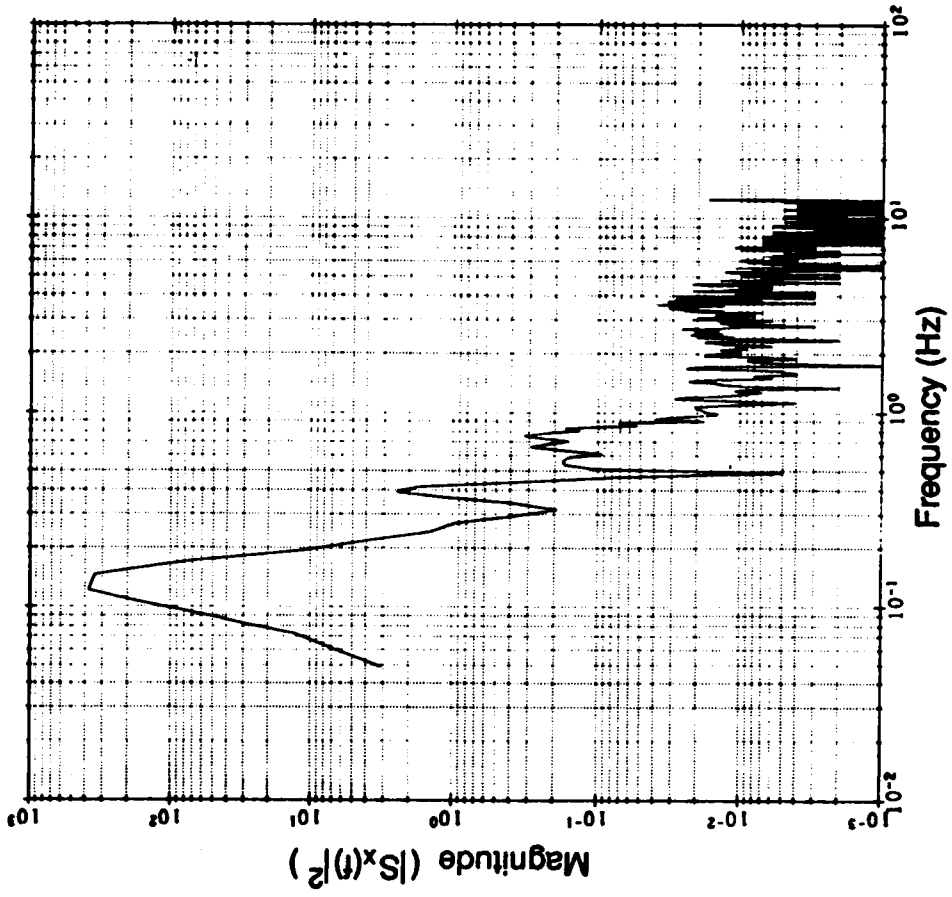
4.3.1 RMS Instrumentation

Existing RMS instrumentation includes joint angle optical encoders to measure joint position, joint tachometers which provide joint rate data and strain gauges (on the instrumented RMS only) to measure boom bending and boom torsion. The encoders are mounted on the gearbox output shaft of each joint, the tachometers are located on the motor output shaft and the strain gauges are mounted near the shoulder pitch and the wrist pitch joints. The encoder and tachometer data is recorded at 12.5 Hz and the strain gauge data is recorded at 25 Hz.

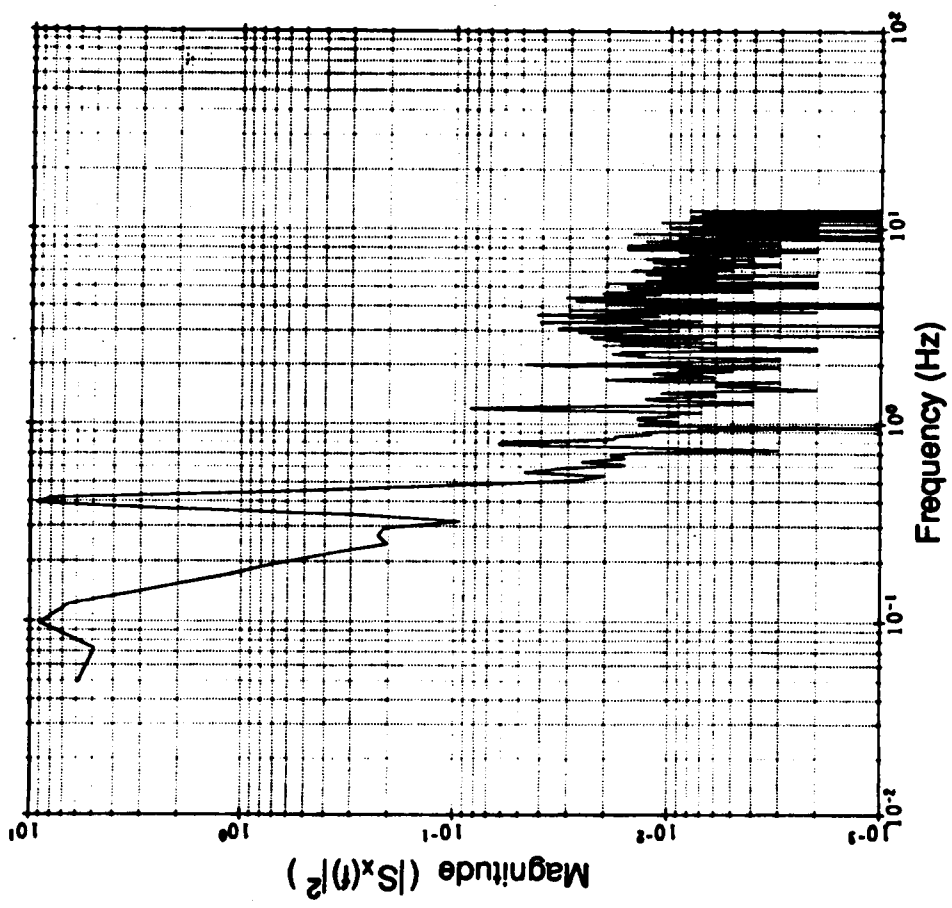
The RMS instrumentation also includes six Closed Circuit Television Cameras (CCTV) (used primarily to facilitate payload handling and to monitor crew activities). Four of the CCTV cameras are located in the cargo bay (forward and aft port bulkheads, aft starboard bulkhead and keel), another is mounted on the roll section of the RMS wrist joint and the final one is on the lower arm boom at the elbow joint. The RMS elbow and wrist cameras can only be controlled and viewed one at a time (serial operation). CCTV coverage can be recorded on a Video Cassette

⁶Level-C data is the name given to mission specific parameter values which are used by the RMS software to 1) calculate joint rates, 2) display position, attitude and rate data and 3) determine system health.

⁷Windler, Milton L., "Baseline PDRS Database," NASA/JSC, March 1988, p.37.



(a) + Wrist Yaw Command



(b) Sinusoidal Wrist Yaw Command

Figure 4.3 Frequency Response of RMS/SPAS System

Recorder (VCR) and/or transmitted to ground via the Orbiter Ku-band communication system. The VCR has a maximum one-hour recording time capability. [8]

Table 4.4 summarizes the granularity, accuracy, resolution, range, data transmission, and data recording characteristics of the RMS instrumentation. [5]

	Granularity	Resolution	Range	Transmission/ Recording	Miscellaneous
ENCODERS	0.0055 deg	—	0 to 360°	12.5 Hz downlist transmission	16 bits available information
TACHOMETERS	0.0879 deg/sec	—	0 to 90 deg/sec	12.5 Hz downlist transmission	12 bits available information
CCTV	—	@ 10ft. 0.2 in. 0.1°	Field of View: 18mm Horiz 39.4° Vert 29.6° 108mm Horiz 6.8° Vert 5.1°	Recording capability Downlist capability	Zoom: 18 - 108 mm Pan: ± 170° Tilt: ± 170°
STRAIN GAUGES	—	Resolution Error ± 0.8%	0 to 500 μ strains	25 Hz on - board recording	—

Table 4.4 RMS Data Acquisition Specifications

In addition to the above instrumentation, the potential may exist to fly the Jet Propulsion Laboratory's (JPL's) Force Torque Sensor on the RMS. The Force Torque Sensor will be sandwiched between the wrist roll joint and the end effector and shall provide force/torque data directly to the crew. Although in its proposed configuration it does not interface with the Orbiter GPC and may not be used real time on-orbit, the Force Torque Sensor data may prove useful as an independent monitor of the experiment and in flight data reduction/analysis. Further, the Force Torque Sensor will probably be flight certified by the time the RMS-Based CSI Flight Experiment is proposed to fly.

4.3.2 SPAS Instrumentation

The attitude control system of the SPAS contains three linear accelerometers and three rate gyros. The linear accelerometers are Sundstrand⁸ QA 1200-AA 08 style accelerometers which have an operating range of 10^{-1} g to 10^{-4} g.⁹ The rate gyros have an attitude rate of $\pm .005$ °/sec accuracy.¹⁰ These six sensors allow formulation of an inertial navigator in the experiment computer to track and provide knowledge of the RMS tip position. This navigator data may be used by performance monitoring and safety algorithms and also to implement tip position controllers.

4.3.3 Modal Displacement Sensors

The advantages and disadvantages of the major instrumentation systems surveyed in this study to augment the existing sensors are summarized in Table 4.5. In terms of technical preference, the most appealing candidates are the fiber optics strain sensor and the accelerometer. Both choices solve the field-of-view or line-of-sight problems which are inherent in optical sensors. In terms of implementation, both of these candidates would also require removal of the RMS thermal blanket for installation of wiring harnesses or optical cables. However, given the ease of implementation and lack of development required, accelerometers were selected as the sensor of choice to measure the modal characteristics of the RMS/SPAS system.

4.3.4 Ku-Band Antenna Dither

It was brought to CSDL's attention that there exists a 17 Hz Ku-Band antenna dither which may saturate the proposed RMS mounted accelerometers.¹¹ This infamous 17 Hz Ku-Band antenna dither was first observed in the Aerodynamic Coefficient Instrumentation Package (ACIP) and Spacelab accelerometer data. The Ku-Band antenna is a dish mounted on a two axis gimbal system which actively tracks Tracking and Data Relay Satellite System (TDRSS), ground stations or target spacecraft. The antenna is dithered at 17 Hz in order to prevent gimbal stiction from interfering with low rate target tracking.¹² The extent to which the 17 Hz oscillation resulting from the antenna dither is transmitted to the RMS is, at this time, unknown. In addition, it remains to be determined whether or not the Ku-Band antenna may be turned off while conducting the

⁸Sundstrand Data Control, Inc..

⁹Messerschmitt-Bölkow-Blohm Specification No. MBB-01.DS.652.0, 10 January 1980, pp. 3-1 - 3-2.

¹⁰Gauthier, J.R., "SPAS-01: Accelerometer Instrumentation," NASA/JSC, 24 June 1982, p. 4.

¹¹Demeo, M. and J. Turnbull, Presentation to NASA/LaRC, "Remote Manipulator System (RMS)-Based Controls-Structures Interaction (CSI) Flight Experiment Feasibility Study: Preliminary Concept," 13 June 1989.

¹²Bergmann, E., "The 17 Hz Solution!," CSDL Memo No. SSV-87-06, 23 February 1987, pp. 1-2.

SENSOR	ADVANTAGES	IMPLEMENTATION PROBLEMS
Accelerometers	<ul style="list-style-type: none"> • No development required • Does not rely on line of sight 	<ul style="list-style-type: none"> • Attachment to RMS • Wires required
Strain Guages	<ul style="list-style-type: none"> • No development required • Does not rely on line of sight 	<ul style="list-style-type: none"> • Attachment to RMS • Wires required
Fiber Optic Strain & Vibration	<ul style="list-style-type: none"> • Does not rely on line of sight 	<ul style="list-style-type: none"> • Attachment to RMS: Under thermal blanket • Development required • Optical cable required • Redundant sensors required
Optical with Active Targets (LEDs)	<ul style="list-style-type: none"> • More accurate than passive targets 	<ul style="list-style-type: none"> • Attachment of targets: On or anchored thru blanket to RMS • Relies on line of sight (limits geometry) • Active targets require wires • Some development required
Optical with Passive Targets (Reflectors)	<ul style="list-style-type: none"> • Successfully used with OAST -1 Solar Array Experiment 	<ul style="list-style-type: none"> • Attachment of targets: On or anchored thru blanket to RMS • Relies on line of sight (limits geometry) • Some modification required
Orbiter Video Cameras	<ul style="list-style-type: none"> • Do not need to make attachments to RMS • Successfully used with OAST -1 Solar Array Experiment • Low technical risk 	<ul style="list-style-type: none"> • Need to adjust focal lengths, aperature and pan-tilt • Trade-Off between resolution and coverage • May not be used for control or safety on orbit
Real-Time Holography	<ul style="list-style-type: none"> • Sensor views entire test article • No targets required • Usable in real-time (5 Hz now, 10 Hz in a couple of years) 	<ul style="list-style-type: none"> • 5 years from space quality • Article needs to be white or silver for good imaging (note: RMS blanket and SPAS thermal jacket are white)

Table 4 .5: Modal Displacement Sensors

experiment.

4.4 Experiment Computer

Two options were considered for the location of the experiment algorithms: in dedicated experiment computers located in the Orbiter cargo bay or in the Orbiter SM GPC. The choice between the two options was primarily dependent on the availability of the SM GPC resources and the speed of the Orbiter GPC.

4.4.1 Computer Speed

An estimation of experiment computer speed requirements was made in order to determine whether the Orbiter GPC is fast enough to do *all* of the experiment computations. The estimation was based upon an estimated number of states, actuators, and sensors (refer to Appendix C: Estimate of Experiment Computer Speed). The results indicated that the experiment algorithms will require from 290k to 1.2M AFLOPS¹³.

The time expended by a single precision multiply and a single precision add of the Orbiter GPC¹⁴ were obtained.¹⁵ Assuming that there was roughly one add associated with each multiply for the multiplication of large matrices (ignoring associated indexing and storage reference operations), the number of AFLOPS accommodated by the GPC was then estimated by adding the number of adds and multiplies. Further, estimating that the SM GPC overhead functions, such as Orbiter fault detection and annunciation and waste water dumps, comprise 25% of the GPC CPU, the available GPC speed was reduced to 86k AFLOPS. After comparing this estimate to the experiment computer speed estimate of 1.2M AFLOPS, it was determined that the experiment computations be performed in experiment computers mounted in the Shuttle cargo bay.

4.4.2 Two Fault Tolerance

In order to facilitate the use of cargo bay mounted experiment computers, the experiment will adhere to existing policy and rationale for the computer based control of hazardous payload systems. [9] These rules mandate that any payload mounted system be two-fault tolerant. This may be achieved by implementing identical, redundant computers, provided that the software is developed by two independent companies. Further, payload safety requirements prohibit the existence of any single point failures on the payload side.¹⁶ Thus, the experiment will employ

¹³Arithmetic Floating-Point Operations Per Sec.

¹⁴These numbers were provided in reference to the new GPC which will be installed in the mid-1990s. The upgrade will increase the memory 2.5x and provide up to 3x the existing processor speed.

¹⁵Somers, Martin (IBM), Telephone Conversation, 11 April 1989.

redundant sensors such that any two sensors could fail without degrading the ability of the experiment computers to detect a violation of performance limits.

The manner by which the experiment computers will be implemented in order to satisfy the two-fault tolerant requirements described is depicted in Figure 4.4. The block diagram depicts two identical computers which are responsible for the data handling, performance monitoring, excitation, and control. Both computers will receive sensor data from the SPAS, RMS, and modal sensors. The excitation and control algorithms are computed in one computer and the computed parameters (i.e. RMS commands and estimator states) are forwarded on to the second computer for recording. Both computers are responsible for performance monitoring of the experiment. Each experiment computer independently checks sensor data and computed parameters to determine if any thresholds have been exceeded. If either computer detects a violation, the experiment is shut down. Our preliminary meetings with the JSC community indicated that this approach was satisfactory.¹⁷

4.4.3 MAST Computers

The computers proposed for use in the RMS-Based CSI Flight Experiment are those which were originally intended for use by LaRC's Control Of Flexible Structures (COFS) program. SCI Technology, Inc., Huntsville, Alabama, is developing both flight qualified and functional equivalent versions of this computer (MAST 1750 A) and it is understood that flight qualification testing of these computers will be completed in early 1990. The computational capacity of these computers (13M AFLOPS) will provide a very comfortable margin above that which will be required by this experiment.

4.5 Carrier Selection

The carriers considered to support the experiment computers and the FMDMs in the Orbiter cargo bay were the Hitchhiker-G, the Spacelab Pallet, and the Multi-Purpose Experiment Support Structure (MPESS) (see Figure 4.5).

The Hitchhiker-G (HH-G) is intended for use as a secondary payload and is designed to mount small payloads to the starboard side of the Orbiter cargo bay. One of two versions of the Hitchhiker, the HH-G can accommodate as many as 6 customer payloads weighing a total of 750 lb..

The U-shaped Spacelab Pallet was designed to fly either with or without the Spacelab pressurized module in the bottom of the Orbiter cargo bay. In the pallet only configurations, subsystem equipment required for the operation of the pallet is housed in the IGLOO which is

¹⁶Demeo, "Preliminary Concept Briefing," pp. 3-4.

¹⁷Ibid., p. 4.

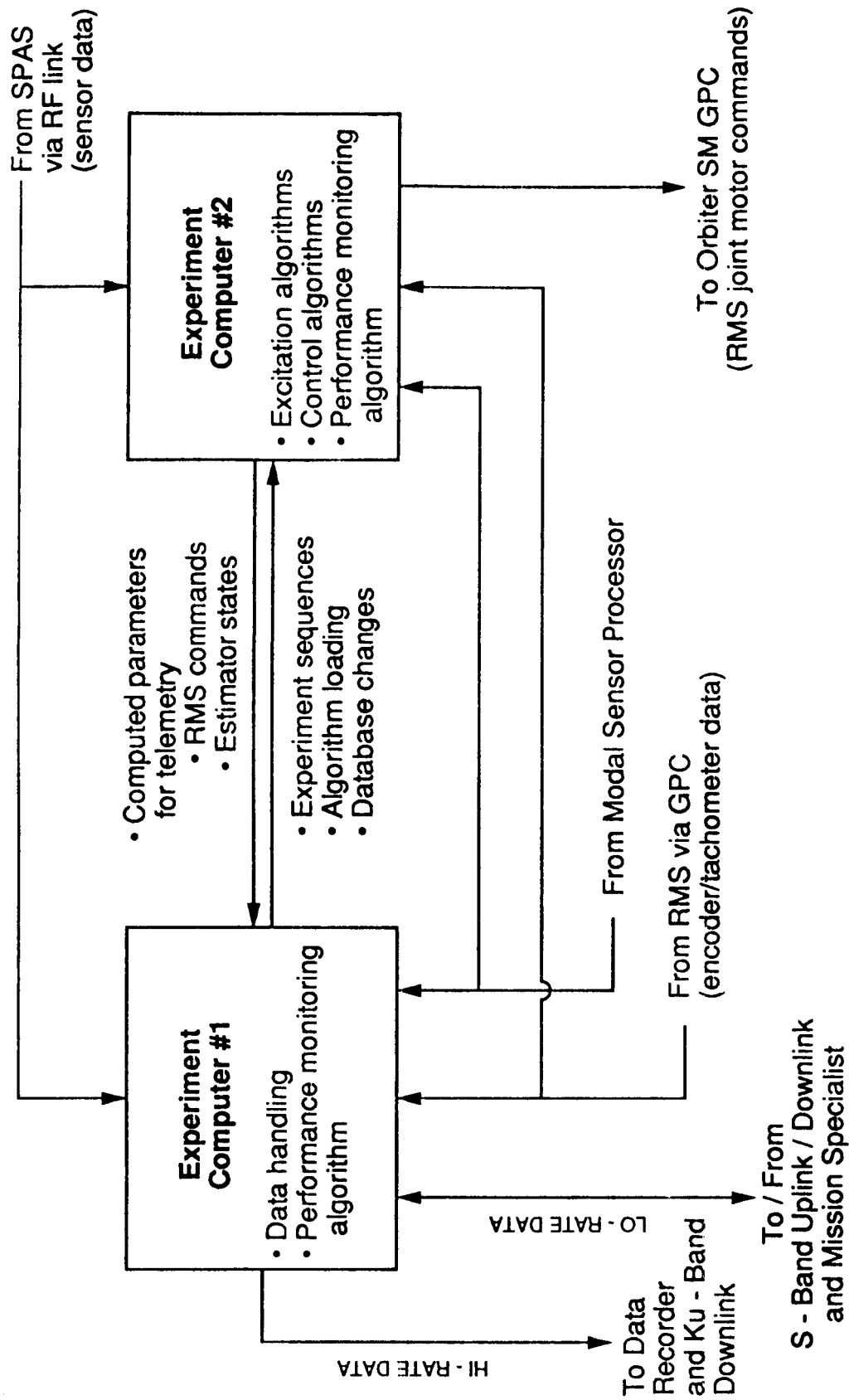
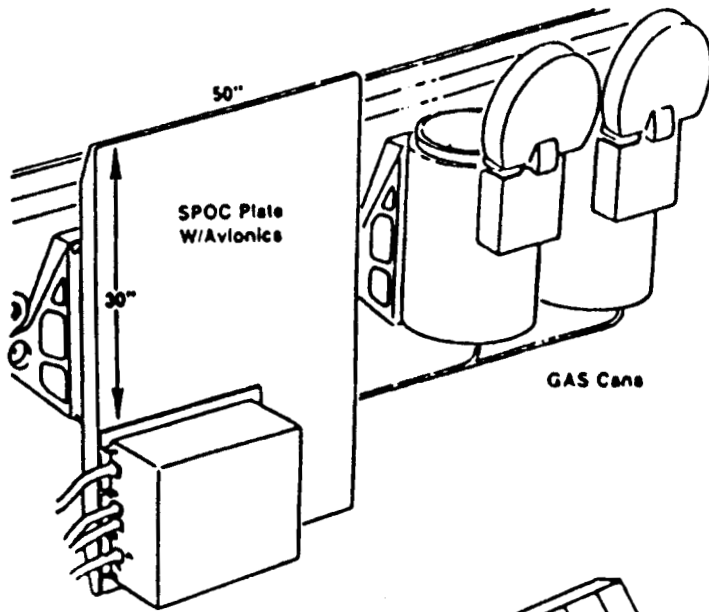
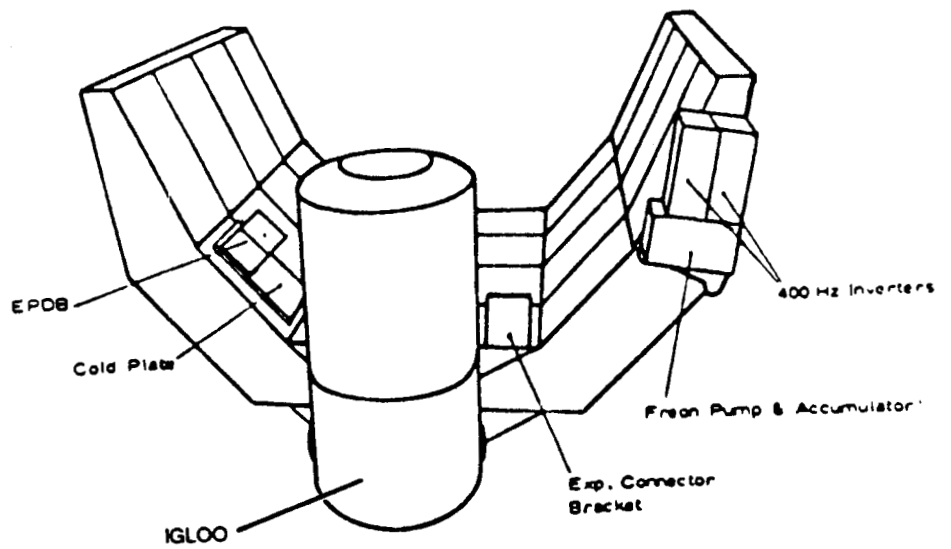


Figure 4.4: Experiment Computer Block Diagram

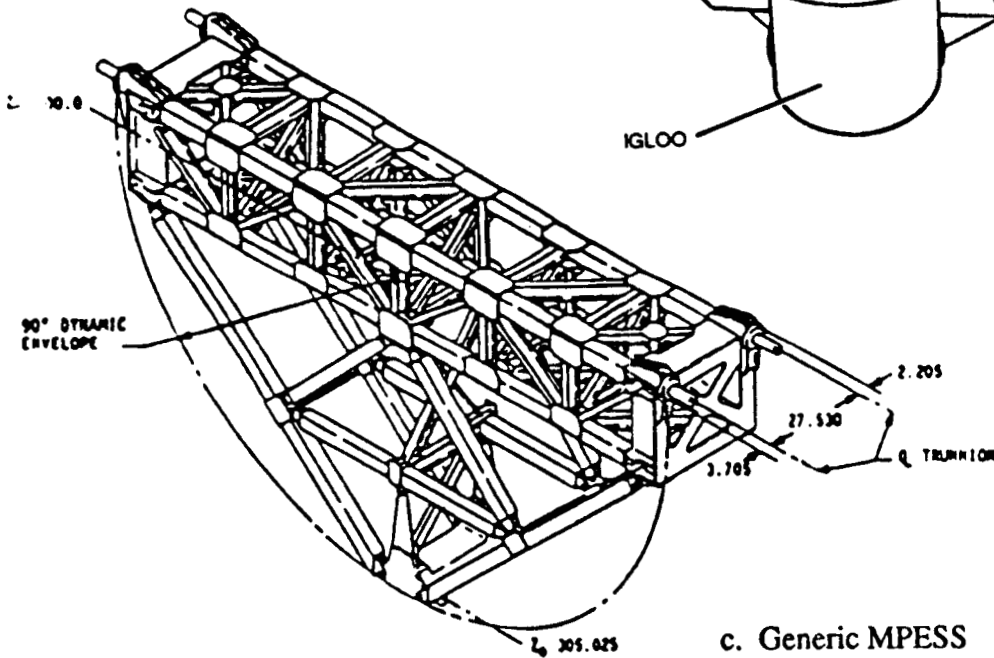
ORIGINAL PAGE IS
OF POOR QUALITY



a. Hitchhiker-G



b. Spacelab Pallet



c. Generic MPRESS

Figure 4.5: Candidate Cargo Bay Carriers

mounted to the front frame of the first pallet section. Pallet configuration may consist of one to five pallet segments.

The MPESS is a Shuttle cross-bay carrier structure which was designed to support unpressurized cargo bay payloads. The MPESS utilizes one quarter of the Orbiter cargo bay resources and may take on various mission configurations such as the Hitchhiker-M which is a cross-bay version of the Hitchhiker payload described above.

The capabilities of these candidate carriers is summarized in Table 4.6.¹⁸

4.5.1 Hitchhiker-G Carrier

The Hitchhiker-G was selected as the carrier of choice primarily because it occupies the minimum Orbiter cargo space while providing adequate power and data rates. The Hitchhiker data management capability easily accommodates the required output of 10 kbps but falls short of the anticipated input requirement of 12 kbps (refer to Appendix D: Orbiter/Carrier Data Rate Estimate). The Hitchhiker input capability can be boosted from 8 kbps to as much as 32 kbps through use of a Medium Rate Multiplexer (MRM).¹⁹ Alternatively, a Flexible Multiplexer Demultiplexer (FMDM) may be used in the Orbiter/Hitchhiker interface (refer to section 4.6.1). The Hitchhiker is also a flight proven and low cost capability for flying the experiment computers and the FMDMs.

4.6 Interface Definition

The general interface requirements for the RMS-Based CSI Flight Experiment are summarized in Figure 4.6. This block diagram depicts the main components of the experiment, namely the SPAS, RMS, SM GPC, modal sensor, and the redundant experiment computers. The carrier mounted experiment computers acquire accelerometer and gyro data from the SPAS, modal sensor data from the RMS mounted modal sensors, joint encoder and tachometer data from the RMS by way of the GPC, housekeeping data and uplinked experiment control parameters. In turn, the experiment computers send joint motor commands to the RMS via the GPC and send selected sensor data, status discretets, housekeeping, estimator states, and modal sensor data to recorders for subsequent downlink and/or mission specialist.

In order to accommodate these communication requirements, the experiment will employ interfaces between (1) the GPC and the RMS (command and telemetry), (2) the SPAS and the GPC (command and telemetry), (3) the SPAS and the experiment computers (telemetry), (4) the GPC and experiment computers (command and telemetry), (5) the recorders and/or mission specialist and the experiment computers and (6) the RMS mounted modal sensors and the carrier

¹⁸Teledyne Brown Engineering MMPF Study Team, "Handbook of Characteristics and Capabilities of STS Compatible Carriers," 15 December 1988, p. 3-35.

¹⁹Dunker, Christopher (NASA/GSFC), Telephone Conversation, 5 September 1989.

CARRIERS	Dimensions External Envelope (ft)	Power		Command Link (kbps)	Data Telemetry Downlink (kbps)	Mass Storage (Mbytes)	
		Available to Users (kW) peak cont.	Total to Carrier (kw) peak cont.				
HITCHHIKER-G	H=5.0 L=10.0	1.3	1.3	1.4	1.4	1300	TBD
MULTI-PURPOSE EXPERIMENT SUPPORT STRUCTURE	H=9.39 W=2.92 L=15.0	1.6	1.6	3.0	1.75	1400	38000 (ETR)
SPACELAB PALLET	L=9.84 W=13.12	8.7 to 9.1	4.4 to 4.8	4.8	4.4	50000	38000 (HARR)

ETR = Experiment Tape Recorder
HARR = High Data Rate Recorder

Table 4.6: Candidate Cargo Bay Carriers

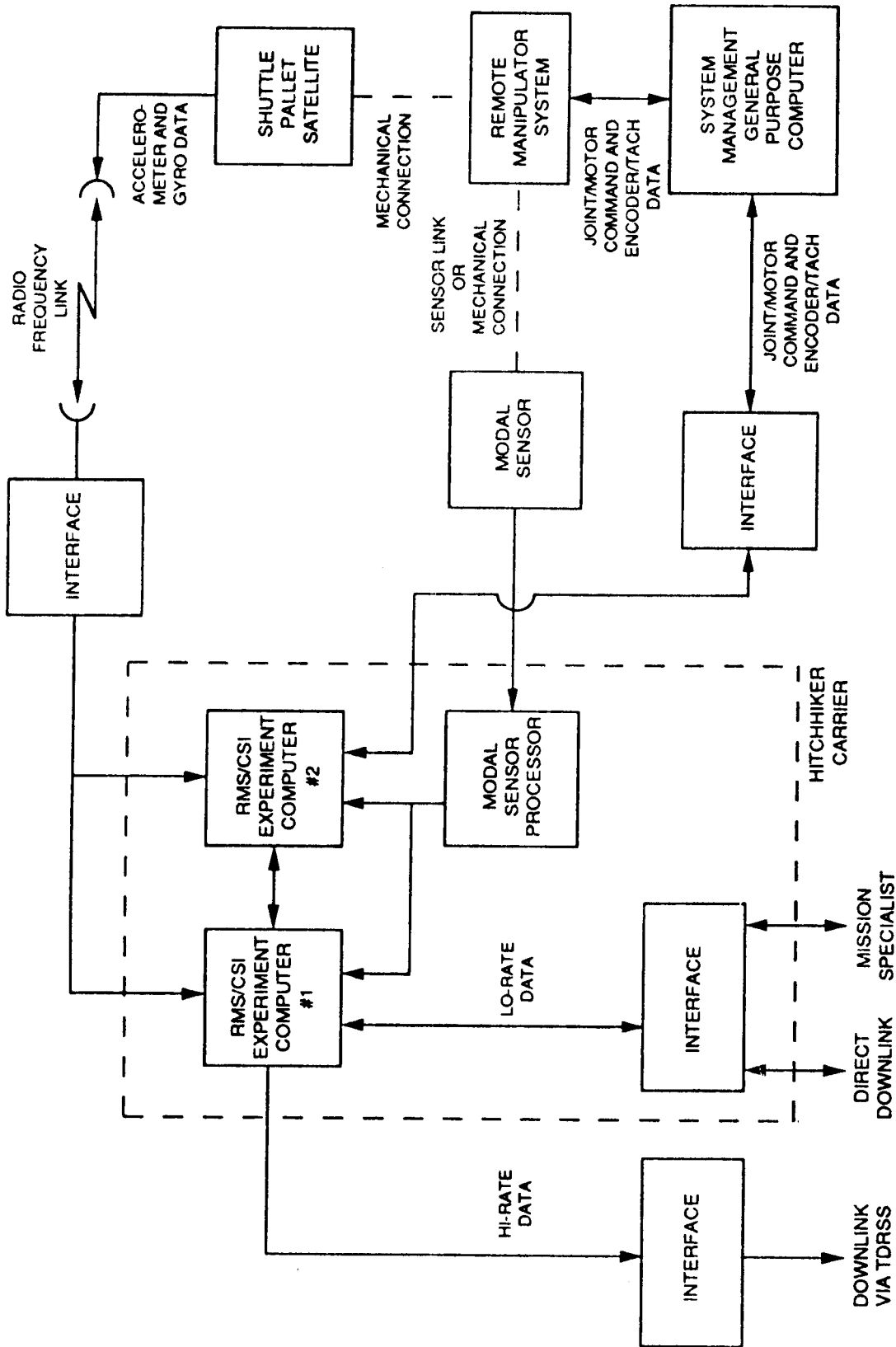


Figure 4.6: General Interface Block Diagram

mounted experiment computers.

The first two of these interfaces are well established and flight proven communication links. The first is provided by the Manipulator Control Interface Unit (MCIU) and the second is accomplished by means of a RF link between a SPAS mounted S-band transponder and the Shuttle Payload Interrogator (PI). [8] The remaining four, to a large extent, hinge upon the choice of cargo-bay carrier to support the experiment computers and FMDMs (refer to previous section). The most difficult of these interfaces to accommodate is that of providing the experiment computers with the authority to command the RMS joint motors via the GPC because, in doing so, the experiment computers must not diminish, violate or bypass any of the existing RMS safety strategies.²⁰

With respect to the cargo bay mounted Hitchhiker, the nominal command interface is via the Payload Signal Processor (PSP) and the nominal telemetry route is via the Payload Data Interleaver (PDI). However, given the substantial amount of interaction which the Hitchhiker mounted experiment computers will have with the Orbiter GPC, it has been established that use of a FMDM interface is warranted.²¹ The FMDM approach minimizes transport delays which may affect controller performance. Instead of sending the data from the SM GPC to the PSP and on to the payload, the data will be sent directly to a FMDM. Telemetry (e.g. RMS joint rate commands) will be sent from the FMDM directly to the SM GPC rather than via the PDI and Pulse Code Modulation Master Unit (PCMMU). The FMDM interfaces with the SM GPC by way of the payload data bus.

The master block diagram of the required interfaces which will be employed by this experiment is furnished in Figure 4.7.

Two of the interfaces depicted, namely, the mechanical attachment of the modal sensors (accelerometers) to the RMS and the routing of the modal sensor data to the Hitchhiker experiment computers, are beyond the scope of standard Shuttle system payload accommodations. Installation of the modal sensors (accelerometers) will require removal of the RMS thermal blanket and perhaps the incorporation of a redundant guillotine to sever the sensor wiring in the event of emergency jettison of RMS. The interface between the (port mounted) RMS fastened accelerometers and the (starboard mounted) Hitchhiker may be provided via the Shuttle Standard Mixed Cargo Harness (SMCH), the Mission Station Distribution Panel (MSDP) and/or the Payload Station Distribution Panel (PSDP). The details of these interfaces will be established during the interface requirements definition of Phase B.

²⁰Demeo, "Preliminary Concept Briefing," pp. 3-4.

²¹Ibid., pp. 2-3.

ACRONYM DEFINITIONS

CMD	Commands
FFMDM	Flight Forward Multiplexer-Demultiplexer
FMDM	Flexible Multiplexer-Demultiplexer
GNC	Guidance, Navigation & Control
GPC	General Purpose Computer
MCDS	Multi-Function CRT Display System
MCIU	Manipulator Control Interface Unit
MMU	Master Memory Unit
MSSDP	Mission Station Distribution Panel
NSP	Network Signal Processor
OPS	Operational
PCM	Pulse Code Modulator
PCMMU	Pulse Code Modulation Master Unit
PDI	Payload Data Interleaver
PI	Payload Interrogator
P/L	Payload
PSP	Payload Signal Processor
PMDM	Payload Multiplexer-Demultiplexer
RCDRS	Recorders
RF	Radio Frequency
RHC	Rotational Hand Controller
RMS	Remote Manipulator System
SIO	Serial Input/Output
SM	System Management
SPAS	Shuttle Payload Satellite
THC	Translational Hand Controller
TLM	Telemetry

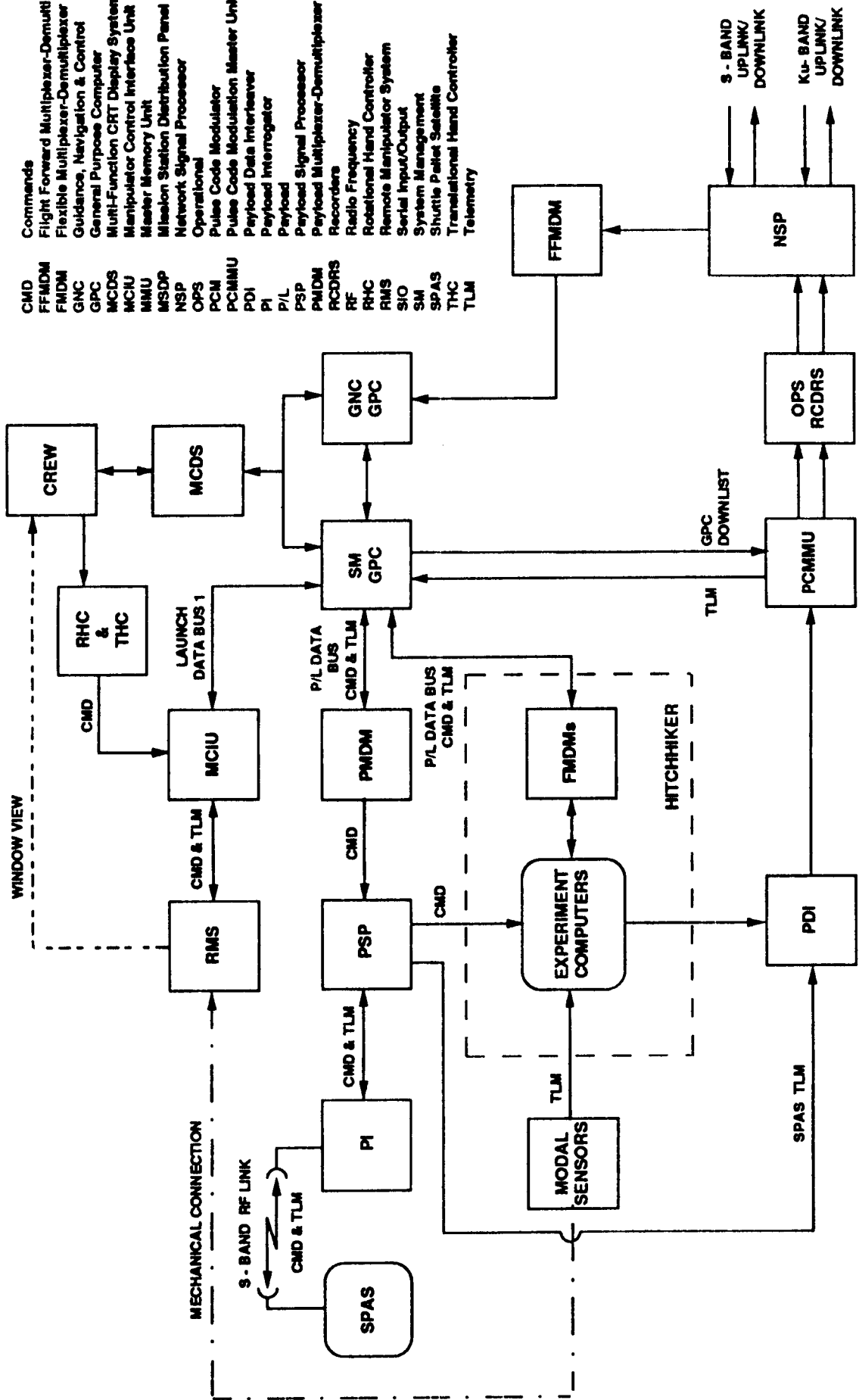


Figure 4.7: Preliminary Interface Block Diagram

4.6.1 Flexible Multiplexer Demultiplexer

The FMDM acts as a data acquisition, distribution, and signal conditioning unit between payloads/carrier and the Orbiter GPC. The FMDM is a commercial version of the Orbiter Multiplexer Demultiplexer (MDM) which is a dual redundant module comprised of a complement of core and Input/Output Modules (IOMs). The FMDM is an Orbiter MDM made up of a set of core modules and eight interchangeable IOMs. The customer typically designs the IOMs per mission requirements and then "plugs" them into an FMDM to support the payload in flight. Thus, the FMDM provides an inexpensive means of configuring MDMs for payload support. The FMDMs are made by Honeywell, Phoenix, Arizona. The FMDMs are generally resident on the payloads themselves and have been used with the Spacelab Pallet, with the MPRESS [10], and with the SPAS⁵.

Due to the existence of single point failures in the FMDM, the experiment will employ two FMDMs to provide the required fault tolerance. These FMDMs will be mounted on the Hitchhiker carrier and will provide interfaces between the experiment computers and the Orbiter GPC as shown in Figure 4.8.

4.6.2 GPC Software Modification

As stated previously, in providing the experiment computer with the authority to command the RMS joint motors, the experiment must not violate, diminish or bypass any of the existing RMS safety strategies, i.e. the System Health Monitor Function (SHMF) or joint rate limits. Establishment of an interface to meet these objectives will require a SM GPC software modification. As with any GPC Change Request (CR) substantial testing in the JSC Shuttle Avionics Integration Laboratory (SAIL) will be required. This will be addressed in section 5.1.

4.7 Safety

4.7.1 RMS Safety Strategies

The RMS/CSI experiment makes maximum use of flight proven RMS safety strategies, procedures, and algorithms. The following is a brief overview of these safety conventions.

The RMS has Built-In Test Equipment (BITE) which assists the crew in the detection of malfunctions and faults of the RMS. When hardware failures occur, the BITE generates flags that alert the RMS operator and ground flight controllers. Rate limits are set in the GPC and are a function of payload mass and inertia. These rate limits are applied to the commands generated by the experiment computer prior to commanding the RMS motors. The System Health Monitor

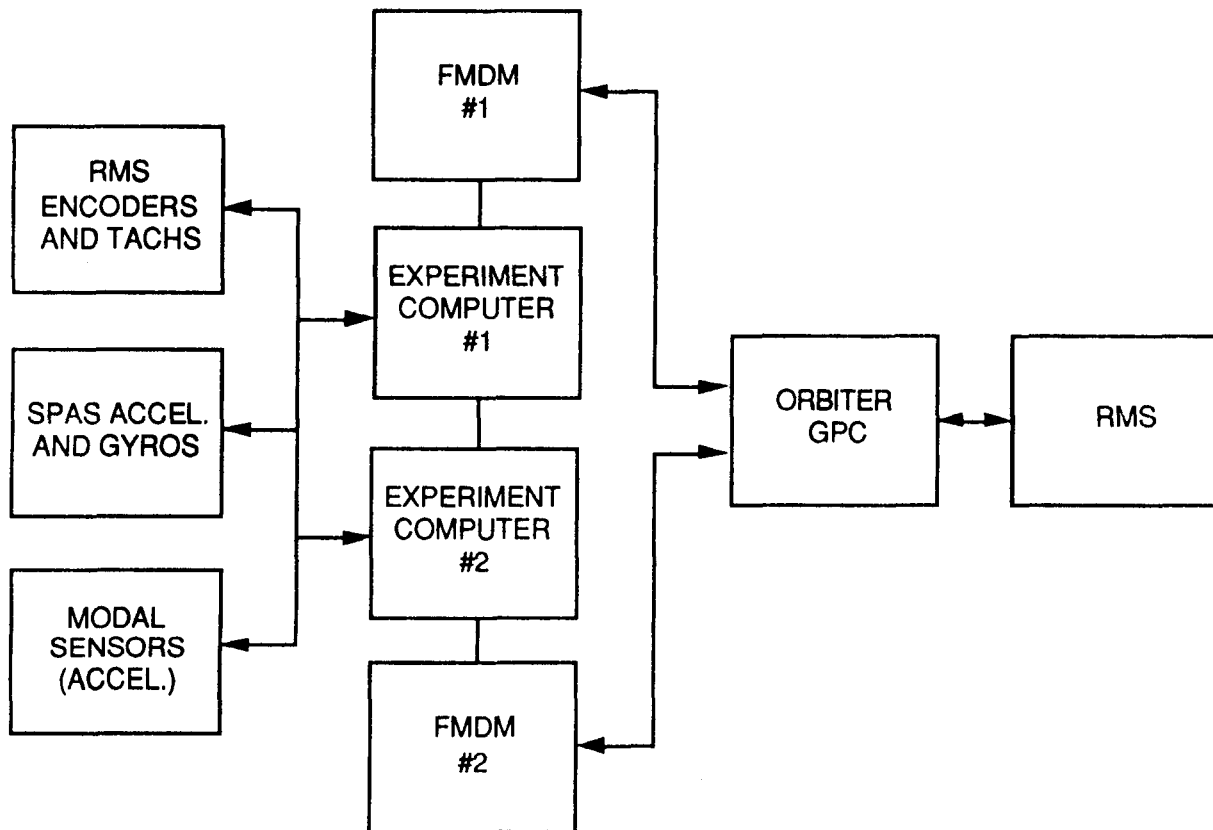


Figure 4.8: Performance Monitoring

Function (SHMF) also resides in the GPC and monitors RMS operational status parameters to detect and annunciate anomalies in the operational status of the RMS. The SHMF is comprised of the following checks which are independent of and in addition to above Rate Limits:

- (a) The Tachometer Data Consistency Check detects joint runaways associated bad tach data by comparing the integrated tach data to *changes* in the position encoder.
- (b) The Rate Envelope Consistency catches joint runaways by comparing actual joint rates against a rate boundary envelope.
- (c) The Position Encoder Check determines the validity of each joint position encoder by comparing the *actual* joint angle to the integrated tach value.
- (d) The Arm Reach Limit ascertains if a joint has exceeded its angular limit.
- (e) The Control Singularity Check detects the loss of one or more degrees-of-freedom of the arm due to the occurrence of a singularity in the arm geometry.

(f) The Uncommanded End Effector Rigidization Check determines if the end effector has derigidized without proper command.

(g) The Uncommanded Payload Release Check detects if the arm has released the payload without proper command.

The RMS structure and joint motors were designed to protect against overloading of the arm. The torque output of the RMS joint motors is limited by a circuit in the servo electronics so as to prevent overloading the RMS structure. In addition, the joint brakes were designed to slip if applied at excessively high velocities in order to avoid an overload condition.

RMS safety procedures include a contingency plan for static failure of the arm assembly. In the extreme, should it be impossible to drive the arm in any of its modes, the arm can be jettisoned to allow the payload bay doors to be closed. The arm may be jettisoned with or without a payload attached.

4.7.2 Experiment Safety Strategies

With consideration to the objectives of the experiment, the following fundamental strategies were established. By adhering to these strategies, it is anticipated that the RMS/CSI experiment will not add any CRIT 1 or CRIT 2 failures.

(1) Absence of dynamic interaction between active DAP and dormant payload of SPAS weight class established by Volume XIV Generic DAP Stability Envelope and by previous flights of the RMS/SPAS.

(2) The Orbiter shall be in free drift during active experiment periods to eliminate the possibility of dynamic interaction between the DAP and experiment control systems.

(3) RMS operating boundaries are restricted to those validated by analyses and previous missions to insure safe dynamic loads.

(4) The crew visually monitors the RMS during experiment periods and may halt undesired motion of the arm by terminating the experiment and applying the brakes.

4.7.3 Collision Avoidance

Consideration has been given to the possibility of unidirectional angular rates of RMS members due to *psychotic* experiment controller phenomena in which the experiment algorithms send unreasonable joint motor rates out to the arm. Collision of the RMS with the Orbiter structure, other payloads, etc. is avoided by conducting the experiment with the maximum clearance to other objects and by providing the following three tiers for detection of anomalous unidirectional motion of the RMS.

FIRST: Experiment Computer Performance Monitoring. These algorithms will be executed in identical, redundant experiment computers. The software, developed by two independent contractors, will use redundant sensor data to check for differences between actual and predicted dynamic performance during the experiment. If either computer detects an out-of-limit condition, the experiment will be automatically shut-down. The performance limits will be set well inside safety limits. Further, the performance monitoring algorithms in the experiment computer will determine the validity of joint rate commands forwarded (via the GPC) to the RMS.

SECOND: SM GPC's Rate Limits. The RMS software will prevent the arm from commanding rates which exceed the payload/joint dependent limits as discussed in 4.7.1.

THIRD: Crew Monitoring. The crew will have the ability to manually shut-down the experiment, apply brakes, and allow the RMS to damp naturally.

4.7.4 Dynamic Fatigue Protection

It was conceived that a growing oscillation mode of failure, caused by controller instability or sinusoidal excitation over long periods, may cause a critical failure of the RMS structure. This oscillatory motion would be caused by *reasonable* commands to the arm which pump energy into the arm. In this case, the commands would not exceed the joint rate limits but they would result in a growing oscillatory motion of the arm.

This experiment mode of failure was simulated using the DRS (refer to Appendix E: Growing Oscillation Mode of Failure). The results verify that the RMS joint servos protect against a growing oscillatory condition and prevent the arm from overloading itself.

Even though the oscillations may not overload the RMS structure, they are of concern since they may shorten the design life of the RMS. The following three tiers of safety are designed to protect against potential dynamic fatigue of the RMS.

FIRST: Experiment Computer Performance Monitoring. These algorithms will check for differences between actual and predicted dynamic performance during the experiment using redundant computers and redundant sensors. If either computer detects an out-of-limit condition, the experiment will be automatically shut-down. The performance limits will be set well inside safety limits.

SECOND: SM GPC's SHMF. It is anticipated that the Rate Envelope Consistency Check of the SHMF would be able to detect growing oscillatory motion of the arm. The Rate Envelope Consistency Check compares the instantaneous actual joint rates against a rate boundary envelope

based on correlated joint rate commands. An out-of-bounds condition for 4 consecutive GPC cycles (4 x 80 msec) constitutes a failure. Thus, the highest (frequency) mode which the consistency check can detect is $(4 \times 0.08) = 0.32$ seconds $\implies 3.125$ Hz. This limit will probably be reasonable given the frequency response of RMS/SPAS system and the fact that the experiment will only try to control the first five modes which appear to fall below 1 Hz.

THIRD: Crew Monitoring. The crew will have the ability to manually shut-down the experiment, apply brakes, and allow the RMS to damp naturally.

4.8 Summary of Preliminary Requirements

4.8.1 Flexible Modes

The RMS/SPAS system was demonstrated to possess several modes below the 1.25 Hz constraint. The number and density of these modes are dependent upon arm configuration and excitation. In the frequency response of the y-axis payload deflection shown in Figure 4.2, there were approximately 4 prominent modes below 1.25 Hz. Thus, it is safe to assume that there will be at least 10 flexible modes in 3 axes below 1.25 Hz. The density and dynamic coupling of modes for different configurations of the RMS should be revisited in Phase B of the experiment. In addition, the excitability and controllability of these modes by the RMS joint motors should be addressed in Phase B.

4.8.2 Payload: SPAS

The flight veteran SPAS payload will provide the required inertial load on the RMS. The 4000 lb. SPAS was designed to accommodate grappling/deployment/recapture by the RMS. The attitude control system of the SPAS also contains linear accelerometers and rate gyros which may be used to sense the tip motion of the experiment system. The operating range and accuracy of these sensors are 10^{-1} g to 10^{-4} g and $\pm .005$ °/sec, respectively. The SPAS possesses suitable data management capabilities, namely, a 5 kbps command rate and an 8 kbps telemetry rate. In addition, the SPAS is equipped with an Ag - Zn battery which supplies 2.38 kW of power.

4.8.3 Actuators: RMS Joint Motors

The flight qualified RMS joint motors possess adequate control authority to excite the RMS/SPAS system. These actuators were designed to protect the structural integrity of the arm and are incapable of damaging the arm (unless the arm is constrained). The capability of these

actuators to excite the first 10 flexible modes of the experiment system and to provide a sensed S/N > 40 dB (100:1) should be addressed in Phase B.

4.8.4 Sensors: Accelerometers

Three accelerometers per axis per upper and lower boom, plus the SPAS and RMS joint sensors should be adequate to characterize the first 10 global flexible modes and to provide redundancy for performance monitoring. The exact number, sensitivity and location of these sensors should be addressed in Phase B. Also, the susceptibility of the accelerometers to the Ku-band antenna dither should also be addressed in Phase B.

4.8.5 Experiment Computer: Cargo Bay Mounted Experiment Computers

The flight qualified COFS MAST computers will be employed and will minimize the cost of the experiment. The computational capacity of these computers, 13 M AFLOPS, will easily accommodate the 290 K AFLOPS to 1.2 M AFLOPS required by the experiment algorithms. These computers will be implemented in a two-fault tolerant manner consistent with JSC/MOD's policy and rationale for the computer based control of hazardous payload systems.

4.8.6 Carrier: Hitchhiker-G

The Hitchhiker is a flight qualified secondary payload which will be used to minimize experiment costs. The data management capabilities of the Hitchhiker (uplink: 8-32 kbps, downlink: 1300-1400 kbps) meet the estimated uplink and downlink required capacities (uplink: 12 kbps, downlink: 10 kbps). The Hitchhiker supplies 1.3 kW of power to the customer. The experiment computers require 25 watts each and the FMDMs receive power from the Orbiter's +28 Vdc power bus via their own power supply system.

4.8.7 Interfaces

The interfaces required to support the experiment were identified as shown in Figure 4.7. The experiment primarily exploits established Shuttle/payload and Shuttle/RMS interfaces. The data rates were found to be sufficient, however, transport delays associated with these interfaces were not investigated. The delays should be addressed in Phase B.

4.8.8 Safety

Existing safety strategies, procedures, and algorithms were augmented to avoid introducing

potential CRIT 1 or CRIT 2 failures. Three tiers of safety, experiment performance monitoring, GPC safety algorithms and crew (manual) shut-off, are used to detect anomalous controller performance, prevent RMS structural overloads, avoid collisions, and detect hardware failures.

Section 5 Test Plans

5.1 Flight Hardware and Software Integration and Testing

Certainly, substantial component (e.g. modal sensors), functional, and environmental qualification/acceptance and safety certification testing to STS specifications will be required. Further, system level integration and testing will be required of (1) Hitchhiker mounted hardware (experiment computers and FMDMs), (2) SPAS mounted modal sensors, (3) RMS mounted modal sensors, (4) experiment computers and (5) GPC software modification. To our advantage, the method of accomplishing many of these integration and test objectives has been well established:

- (1) The HH-G Project Office at GSFC (with customer support) typically provides for the integration of the customer's payloads onto the Hitchhiker and performs system functional, Electromagnetic Interference (EMI), and Flight Acceptance tests. [11]
- (2) It is anticipated that the SPAS payload will be shared and that the majority of the integration and testing procedures will be born by the primary customers.
- (3) SPAR Aerospace would undertake the installation of the modal sensors on the RMS, functional integration and flight qualification of the modified arm.
- (4) The burden of flight qualifying the experiment computers will be alleviated by employing computers which were originally developed for LaRC's COFS program (refer to section 4.4). With respect to experiment computer software, software module (unit level) testing and integrated (subsystem level) testing will be needed.
- (5) JSC's Shuttle Avionics Integration Laboratory (SAIL) provides the facility for system level integration and testing of experiment hardware and software that interfaces with the operational system (mainly the GPC).

With respect to this last item, it has been established that the experiment will require nonroutine SAIL testing on account of the fact that the experiment system will interface with the Orbiter operational system. Specifically, the experiment computers will interface with the SM GPC for the purposes of acquiring sensor data and experiment control parameters and in order to send joint control commands to the RMS and to record sensor data and estimator state parameters for subsequent downlink. Testing and verification of these interfaces will be an extremely complex task requiring several new math models, modifications of flight software, SAIL hardware modifications and possible flight hardware/mission kit modifications/installations.

The math models and simulations required for SAIL testing include the following:

- (1) Modeling of RMS mounted modal sensors (accelerometers) via the Vehicle Dynamic Simulation (VDS)
- (2) Modeling Shuttle Pallet Satellite (SPAS) sensors (accelerometers and gyros) via

the Payload Avionics Test Station (PATS)

- (3) Simulation of the SPAS/Payload Interrogator (PI) Radio Frequency (RF) link
- (4) Simulation of the interface between modal sensors and experiment computers
- (5) Simulation of the interface between the Hitchhiker and the SM GPC

The Hitchhiker-G avionics integrated (by GSFC) with experiment hardware will be brought to JSC for use in SAIL testing. The experiment hardware consists of redundant functional equivalent experiment computers and a pair of functional equivalent FMDMs. Although it has been established that SAIL has the facility to simulate an FMDM, for the purposes of this study (e.g. cost estimates) it is assumed that functional equivalent versions of the FMDM will be supplied for use in SAIL testing.

5.2 On-Orbit Testing

The aforementioned differences between CSI control techniques and conventional methods and the inevitable uncertainties in extrapolating ground test results to on-orbit environments will make on-orbit testing a necessity. On-orbit testing of the RMS/SPAS system will be conducted in a two flight scenario. On the first flight, characterization of the RMS/SPAS system will be performed and during the second flight, 6 months later, an abbreviated characterization followed by vibration suppression experiments will be conducted. Identical hardware will be used on the first and second flights with the possible exception of slightly different mass properties of the SPAS due to the evolving needs of the co-user of the SPAS.

Excitation and characterization of the flexible modes of the RMS/SPAS below 1.25 Hz for several different configurations of the arm will be executed on the first flight. Post-flight, the modal data will be analyzed and the results used to update the system models. Predictions will then be made of the controller performance during the experiments and the performance monitoring algorithms in the experiment computers will be updated.

On the second flight a repeat of selected characterization tests will be performed to identify any changes from the first flight. The modal data will be processed overnight and the controller parameters updated and uplinked as required. The control experiments will then be conducted in a conservative progression: (a) vibration suppression in several fixed RMS configurations, (b) single axis, single member articulation experiments with vibration suppression, and (c) multi-axis, multi-member articulation experiments with vibration suppression.

Section 6

Schedule Estimate

6.1 Approach

The approach used in formulating schedule estimates for the RMS-Based CSI Flight Experiment was to partition the experiment into four phases: (1) Phase A: Feasibility Study (completed), (2) Phase B: Experiment Definition, (3) Phase C/D: Design Synthesis and Development, and (4) Post Flight Analysis. Further, the master experiment schedule was broken down into a series of subschedules. The nine subschedules which were defined include: (1) Algorithm Design, (2) Modal Sensor, (3) Hitchhiker, (4) GPC Software Modification, (5) RMS Modification, (6) Experiment Computer, (7) Mission Operations Development, (8) Verification, and (9) Second Flight.

The task timelines were estimated using information based upon the relationship between experiment/payload development and the payload integration process and payload documentation timelines established by NASA. [8]

6.2 Results

The resulting master schedule spans a five year period. As shown in Figure 6.1, the first year is devoted to Phase B: Experiment Definition, followed by three years of Phase C/D: Design Synthesis and Development and a year of Phase E: Post Flight Evaluation. The schedules for Phases B and Phase C/D are given in Figures 6.2 and 6.3, respectively. The subschedules are provided in Appendix F.

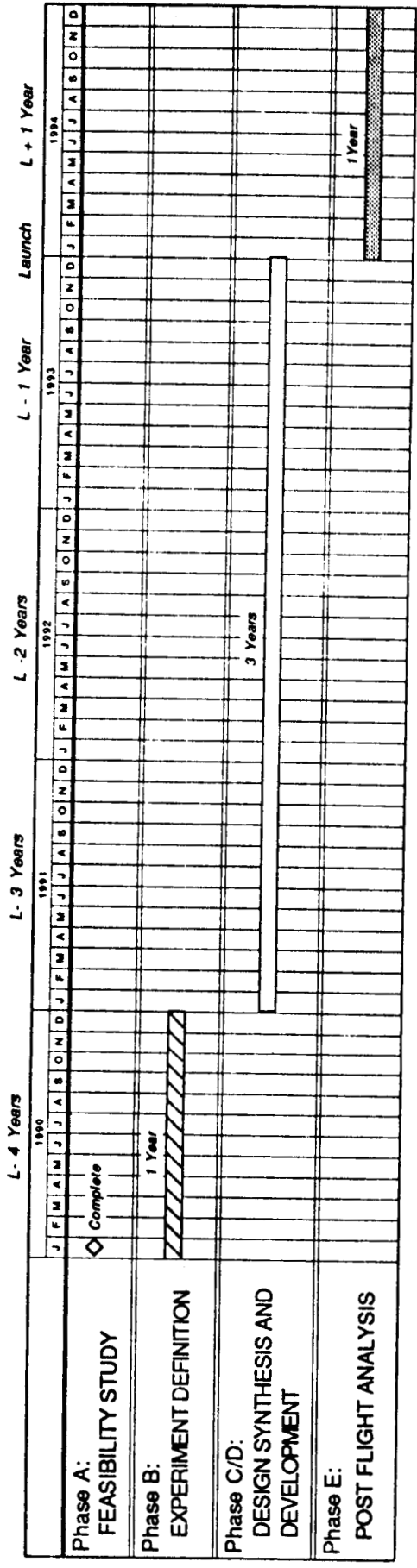


Figure 6.1: Master Milestone Schedule

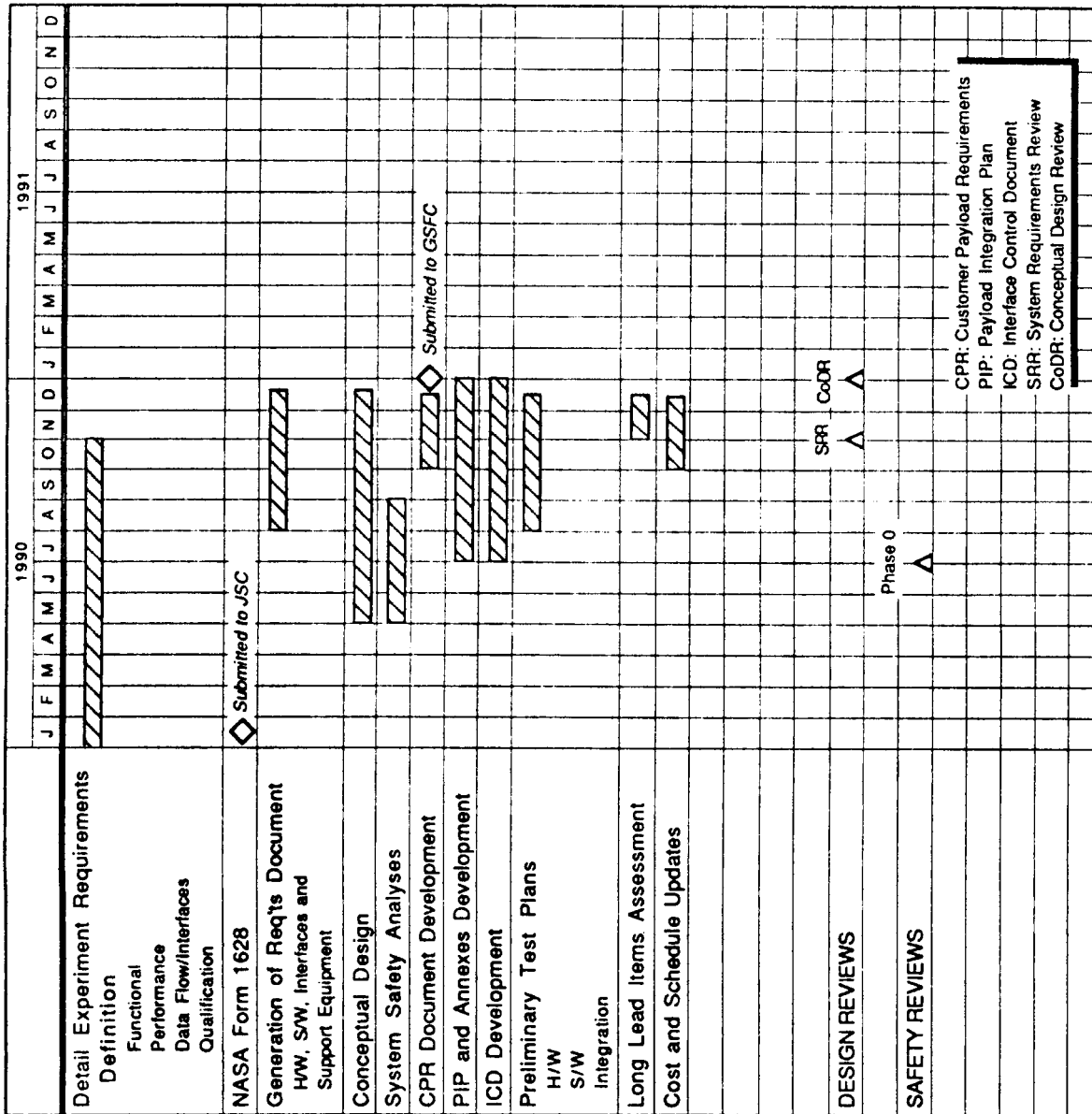


Figure 6.2: PHASE B - Experiment Definition

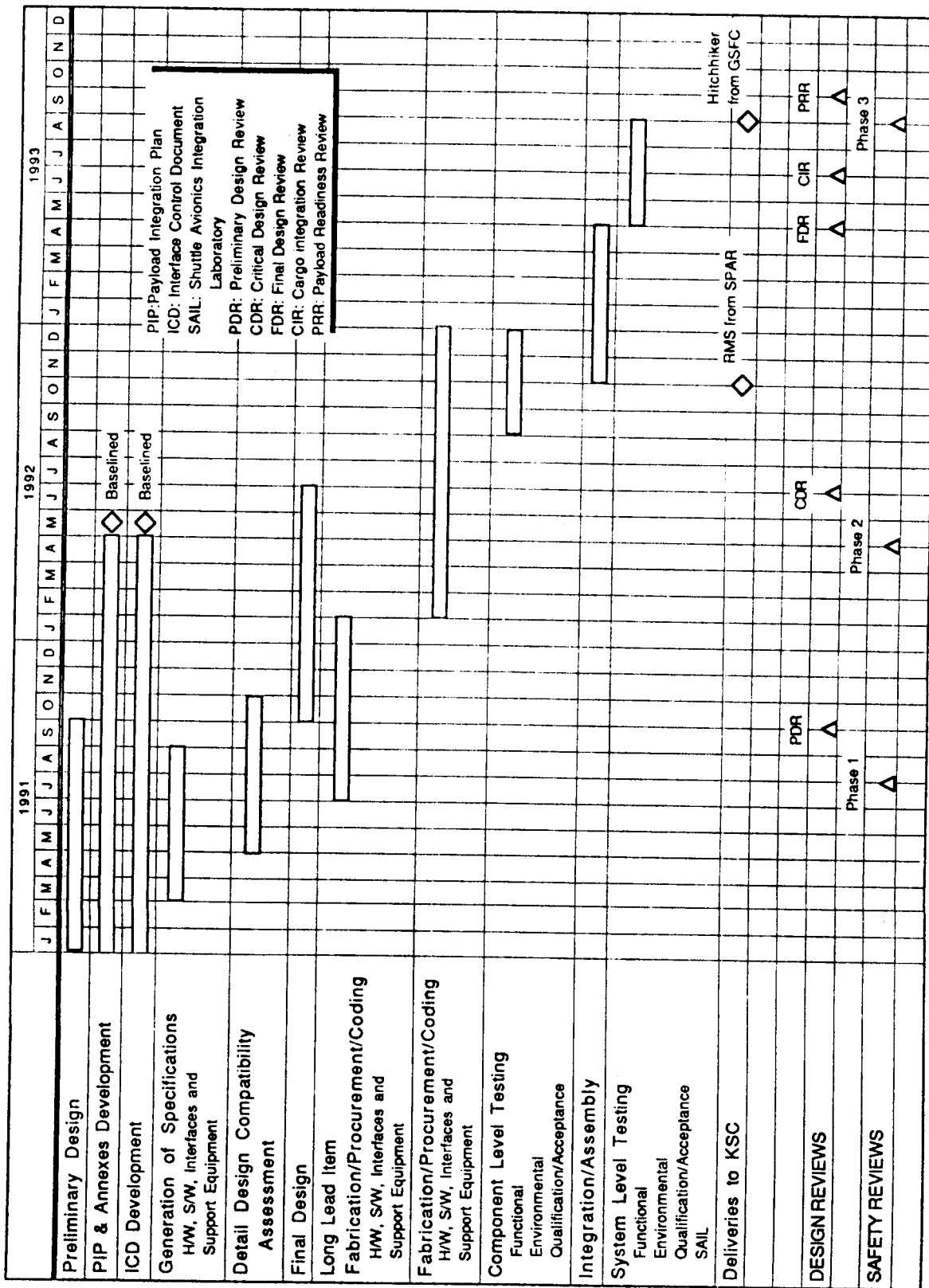


Figure 6.3: PHASE C/D - Preliminary Design Synthesis and Development

Section 7 Cost Estimate

7.1 Approach

The cost estimate was based upon the level of effort required to support the subschedules defined in the previous section. Standard transportation costs, e.g. launch, payload deployment, etc., for flying the SPAS and Hitchhiker payloads are not included. Further, it is assumed that the rental costs for both the SPAS and the Hitchhiker by a NASA agency are absorbed in these standard transportation costs. The cost estimates are for the two flight scenario described in section 6 and are in 1989 dollars unless otherwise indicated. The Modal Sensor Subschedule hardware costs were based upon the use of accelerometers as the baseline RMS mounted modal sensors.

7.2 Results

The cost estimates for the nine subschedules in terms of engineering support, experiment unique hardware and total cost are summarized in Table 7.1. The total cost of the two flight experiment is estimated at \$27.6 M. The highest price tag is attached to the experiment computer subschedule at \$10.8 M which is 39.1% of the total cost and 42.6% of the total engineering cost. This is a result of the substantial cost incurred in software development, testing, and documentation. The second highest total cost is associated with the mounting of accelerometers on the RMS at \$5 M.²² The third highest total cost belongs to the Hitchhiker subschedule. The experiment hardware included in this subschedule consists of two flight qualified FMDMs, two functional equivalent FMDMs²³, Hitchhiker avionics and ground support equipment²⁴. The estimated cost of this hardware is \$3.7 M which is 50.7% of the total cost of experiment unique hardware.

The cost break down in terms of experiment phases is provided in Table 7.2. The Phase B costs amount to 6.3% of the Phase C/D cost. The cost associated with Phase C/D comprises 94.1% of the total experiment cost.

7.3 Factors That Tend to Minimize Cost

There are several factors which tend to minimize the cost of this on-orbit CSI experiment:

²²Per estimate from SPAR Aerospace via Elizabeth Bains (NASA/JSC), September 1989.

²³Per estimate from J.C. Kinker, Honeywell Inc., Space Systems Group, Glendale, Arizona, September 1989.

²⁴Per estimates from Clarke Prouty and Christopher Dunker, Hitchhiker Project Office, NASA Goddard Space Flight Center, Greenbelt, Maryland, September 1989.

- (1) A flight qualified flexible test article exists (RMS) which has a flight proven operational capability and safety strategy. Further, procedures for RMS modification exist via the SPAR support contract to NASA/JSC.
- (2) A flight qualified payload which possesses flight proven safety strategies, release/recapture mechanisms, RF data link and sensors (to form inertial navigator for end position control and safety strategy) exists (SPAS). In addition, SDIO owns a SPAS and is willing to share it with NASA on a future flight.
- (3) The GSFC supports standard integration and testing of the Hitchhiker carrier at no cost to a NASA organization.
- (4) Procedures for GPC software modification, i.e. a software Change Request (CR), are well established via an IBM support contract to NASA/JSC.
- (5) The facility for system-level integration and testing of the experiment hardware, software, and interfaces exist (JSC/SAIL).
- (6) The experiment computers will be flight qualified in early 1990 as a fallout of LaRC's COFS program. Flight units and functional equivalent units can then be purchased from SCI Technology, Inc. at reasonable prices.

SUBSCHEDULE	ENGINEERING	EXP UNIQUE HARDWARE	TOTAL COST
ALGORITHM DESIGN	1,042.	0.	1,042.
MODAL SENSOR	433.	100.	533.
HITCHHIKER	1,017.	3,650.	4,667.
GPC SOFTWARE MODIFICATION	1,150.	0.	1,150.
RMS MODIFICATION	5,333.	0.	5,333.
EXPERIMENT COMPUTER	8,700.	2,100.	10,800.
MISSION OPERATIONS DEVELOPMENT	433.	0.	433.
VERIFICATION	900.	1,000.	1,900.
SECOND FLIGHT	2,000.	0.	2,000.
TOTAL	21,008.	6,850.	27,858.

TABLE 7.1: Subschedule Cost Summary (\$ K)

SUBSCHEDULE	PHASE B	PHASE C/D	TOTAL COST
ALGORITHM DESIGN	492.	550.	1,042.
MODAL SENSOR	283.	250.	533.
HITCHHIKER	434.	4,233.	4,667.
GPC SOFTWARE MODIFICATION	50.	1,100.	1,150.
RMS MODIFICATION	100.	5,233.	5,333.
EXPERIMENT COMPUTER	267.	10,533.	10,800.
MISSION OPERATIONS DEVELOPMENT	0.	433.	433.
VERIFICATION	0.	1,900.	1,900.
SECOND FLIGHT	0.	2,000.	2,000.
TOTAL	1,626.	26,232.	27,858.

Table 7.2: Cost Summary (\$ K)

Section 8

Conclusions and Recommendations

The RMS-Based CSI Flight Experiment will enable the advancement of CSI technology through the demonstration of on-orbit characterization and flexible-body control of large space structure dynamics. The Shuttle RMS with an attached payload is a viable test article because it is capable of large angle articulation of flexible members which are difficult to characterize using ground test techniques.

In addition, by utilizing existing hardware the experiment minimizes the costs and risk of implementing a flight experiment. The RMS, SPAS, and Hitchhiker are flight qualified systems which have well established integration, operation, and safety strategies. Further, although specially designed test structures could be better instrumented and less complicated than the RMS, an RMS-based experiment would be less costly to implement.

The experiment also offers the promise of spin-off enhancement to the Shuttle RMS and Space Station RMS. The potential for improvement exists in the handling of heavy and/or flexible payloads, Orbiter DAP performance and space station assembly. With respect to the Orbiter DAP, it is anticipated that suppressed modal vibrations will reduce dynamic coupling with the DAP and will increase stability margins. With respect to space station assembly, it is anticipated that the experiment controller would suppress the oscillations of the RMS/payload system which add time to payload deployment, retrieval, and maneuvering.

During this study, the attendees of various presentations and briefings at CSDL, JSC, LaRC and NASA Headquarters have suggested the following additional research:

- (1) Employ a flexible payload on the RMS rather than the relatively rigid SPAS payload and demonstrate the ability of CSI controllers to suppress both RMS and flexible payload dynamics.
- (2) Operate the DAP and the RMS, with a heavy payload, simultaneously to quantify the increase in DAP stability margins produced by the CSI controller.
- (3) Examine feasibility of reducing the order of the CSI control laws such that they may be implemented in the Orbiter GPC. Control of a single flexible mode may provide significant performance improvement.

Section 9

Acknowledgements

The work documented in this report was supported by funds provided by the National Aeronautics and Space Administration Langley Research Center and administered under contracts NAS9-17560 and NAS9-18147. Acting as joint task monitors for the study were Mr. Anthony Fontana of the Langley Research Center and Dr. Elizabeth Bains of the Johnson Space Center.

The author would like to thank both task monitors and Joseph Turnbull of CSDL for their contributions to the work documented in this report.

Section 10 References

- [1] "NASA/DOD Controls-Structures Interaction Technology 1989," NASA-CP-3041, Conference Proceedings, San Diego, CA, 29 January - 2 February 1989.
- [2] Bole, Catherine D. and Rhonda R. Foale, "RMS Mission Histories," NASA JSC-23504, March/April 1989, p. 13 and p.16.
- [3] Sargent, Darryl G., "Impact of Remote Manipulator Structural Dynamics on Shuttle On-Orbit Flight Control," AIAA-84-1963, AIAA Guidance and Control Conference, Seattle, Washington, 20-22 August 1984.
- [4] "Shuttle Flight Operations Manual; Volume 16 - Payload Deployment and Retrieval System," NASA JSC-12770, Flight Operations Directorate, Crew Training and Procedures Division, 1 June 1981.
- [5] Lepanto, Janet A., "Remote Manipulator System/Large Space Structure RTOP, Final Report," CSDL-R-1755, 18 December 1984.
- [6] Gray, C. et al., "Validation of the Draper RMS Simulation (DRS) Against Flight Data," CSDL-R-1777, Volumes 1-2, April 1985.
- [7] Bailey, T., Gruzen, A., and P. Madden, "RCS/Linear Discrete Actuator Study," CSDL-R-2075, AFAL-TR-88-039, August 1988.
- [8] "Space Shuttle System Payload Accommodations," NSTS-007700, NASA/JSC, Volume XIV, Revision J, 27 January 1988.
- [9] "Safety Policy and Requirements for Payloads Using the National Space Transportation System (NSTS)," NSTS 1700.7B, NASA/JSC, January 1989, p. 11.
- [10] Schock, Richard W., "Solar Array Flight Dynamic Experiment," NASA Technical Paper 2598, 1986.
- [11] "Hitchhiker Shuttle Payload of Opportunity Carrier Customer Accommodations and Requirements Specifications," HHG-730-1503-04, Preliminary Revision, NASA/GSFC, July 1988, pp. 3-15 - 3-16.

Appendix A: Acronym Definition

ACIP	Aerodynamic Coefficient Instrumentation Package
AFLOPS	Arithmetic Floating Point Operations Per Sec
BITE	Built-In Test Equipment
CCTV	Closed-Circuit Television
CMD	Command
CMG	Control Moment Gyro
COFS	Controls Of Flexible Structures
CPU	Central Processing Unit
CSDL	The Charles Stark Draper Laboratory, Inc.
CSI	Control-Structures Interaction
DAC	Data Acquisition Cameras
DAP	Digital Auto Pilot
DRS	Draper RMS Simulation
ELP	Elbow Pitch
EMI	Electromagnetic Interference
FCS	Flight Control System
FFMDM	Flight Forward MDM
FFT	Fast Fourier Transform
FMDM	Flexible MDM
GAS CAN	Get Away Special Canister
GNC	Guidance, Navigation, and Control
GPC	General Purpose Computer
GSFC	Goddard Space Flight Center
HH-G	Hitchhiker-G
Hz	Hertz
IOM	Input/Output Module
JPL	Jet Propulsion Laboratory
JSC	Johnson Space Flight Center
LaRC	Langley Research Center
MBB	Messerschmitt-Bölkow Blohm
MCDS	Multi-Function Cathode Ray Tube (CRT) Display System
MCIU	Manipulator Control Interface Unit
MDM	Multiplexer Demultiplexer
MMU	Master Memory Unit
MPSS	Multi-Purpose Experiment Support Structure
MPM	Manipulator Positioning Mechanism

MRM	Medium Rate Multiplexer
NCR	None Compliance Report
NSP	Network Signal Processor
OBAS	Orbiter Body Axis System
OPS	Operations
PCM	Pulse Code Modulation
PCMMU	PCM Master Unit
PDI	Payload Data Interleaver
PDRS	Payload Deployment and Retrieval System
PFTA	Payload Flight Test Article
PI	Payload Interrogator
PL MDM	Payload MDM
PMA	Proof-Mass Actuator
POR	Point Of Resolution
PRCS	Primary Reaction Control System
PSP	Payload Signal Processor
RCDRS	Recorders
REM	Release Mechanism
RF	Radio Frequency
RHC	Rotational Hand Controller
RMS	Remote Manipulator System
SAIL	Shuttle Avionics Integration Laboratory
SDIO	Star-Wars Defense Initiative Office
SFSS	Spartan Flight Support Structure
SHP	Shoulder Pitch
SHY	Shoulder Yaw
SIO	Serial Input/Output
SM	Systems Management
SMCH	Standard Mixed Cargo Harness
SPAS	Shuttle Pallet Satellite
STS	Space Transportation System
TDRSS	Tracking and Data Relay Satellite System
THC	Translational Hand Controller
TLM	Telemetry
VCR	Video Cassette Recorder
WRP	Wrist Pitch
WRR	Wrist Roll
WRY	Wrist Yaw

Appendix B: Proof-Mass Actuator Sizing

The following is an estimate of the size PMA which would be required, in terms of mass and stroke, to support the RMS-Based CSI Flight Experiment. This formulation predicts the steady state force required to pump the RMS/SPAS system to a reasonable excitation amplitude.

Consider the following dynamics of a single degree-of-freedom system:

$$m_g \ddot{x} + kx + c\dot{x} = F$$

or,
$$m_g \ddot{x} + \omega^2 m_g x + 2\xi \omega m_g \dot{x} = F \quad (\text{b.1})$$

where F = amplitude of sinewave actuator force
 m_g = effective mass (SPAS mass $< m_g <$ (SPAS + RMS) mass)
 ξ = natural damping of RMS
 $\omega = 2\pi f$
 k = stiffness coefficient
 c = damping coefficient
 x, \dot{x}, \ddot{x} = displacement, velocity, acceleration of effective mass

Further, assume simple harmonic motion, i.e.

DISPLACEMENT
$$\begin{aligned} x(t) &= A \sin \omega t \\ |x(t)|_{\text{peak}} &= A \end{aligned} \quad (\text{b.2})$$

VELOCITY
$$\begin{aligned} |\dot{x}(t)| &= \omega A \cos \omega t \\ |\dot{x}(t)|_{\text{peak}} &= \omega A \end{aligned} \quad (\text{b.3})$$

ACCELERATION
$$\begin{aligned} |\ddot{x}(t)| &= -\omega^2 A \sin \omega t = -\omega^2 x(t) \\ |\ddot{x}(t)|_{\text{peak}} &= -\omega^2 |x(t)|_{\text{peak}} = -\omega^2 A \end{aligned} \quad (\text{b.4})$$

where A = amplitude of sinewave RMS tip deflection

Substituting equations b.2, b.3, and b.4 back into the dynamics equation, b.1, yields:

$$-m_g \omega^2 A + \omega^2 m_g A + 2\xi \omega m_g \omega A = F$$

Thus,

$$F = 2\xi\omega^2 m_g A$$

or,

$$F = \frac{2\xi\omega^2 m_g A}{\phi^2} \quad (b.5)$$

where ϕ = influence coefficient; influence of actuator to be excited.

This formula applies after sinusoidal excitation to steady state deflection and gives the actuator force amplitude required to balance RMS damping at a given deflection.

Let $m_g = 4500$ lbs. ($4000 < m_g < (4000+1000)$)

$\xi = 3\%$

$\omega = 2\pi f$; $f = 0.1$ Hz

$\phi = 1$; actuator located at tip of RMS at point of maximum modal deflection of first bending mode

and $A = 6$ in.

$$F = 2\xi\omega^2 m_g A$$

$$F = 2(0.03)(0.39)(4500)(0.5) = 52.65 \text{ lbft/sec}^2 \quad (b.6)$$

$$\Rightarrow 1.64 \text{ lbm}$$

Now, substituting the peak value of acceleration, eqn. b.4, into Newton's 2nd law:

$$F = ma = m\omega^2 s$$

where F = amplitude of sinewave actuator force

m = moving mass of actuator

$\omega = 2\pi f$

and s = amplitude of sinewave stroke of actuator

Using $F = 52.65 \text{ lbft/sec}^2$ from eqn b.6 and arbitrarily choosing $m = 100 \text{ lbm}$ and $f = 0.1$ Hz and solving for actuator stroke:

$$s = \frac{F}{m\omega^2} = \frac{52.65}{(100)(0.39)} = 1.35 \text{ ft}$$

Thus, the peak-to-peak stroke would be 2.7 ft.

Alternatively, doubling the proof-mass, $m = 200$ lbm, the required stroke would be:

$$s = \frac{F}{m\omega^2} = \frac{52.65}{(200)(0.39)} = 0.68 \text{ ft}$$

This has reduced the stroke length at the cost of increasing the proof-mass to 200 lbs. This is characteristic of the trade-off between the size of the actuator proof-mass and stroke length.

A proof-mass actuator of this size is not an off-the-shelf item. Development of an actuator for this application would be a formidable task in itself. It is also too large and heavy to be a practical actuator for realistic applications. Further, a PMA of this size may be capable of causing dynamic failure of the RMS.

Appendix C: Estimate of Experiment Computer Speed

◇ From FFT plots of RMS/SPAS data (Figures 4.2 and 4.3), it is evident that as many as 4 flexible-body modes occur in the X-axis within 1.25 Hz. Thus, it is assumed that there will be approximately 10 flexible-body modes in 3-axes below 1.25 Hz.

◇ State Estimator Strategy

- If 5 flexible-body modes are to be controlled, should estimate 10 flexible-body modes (spillover)
- Estimate 6 rigid-body modes and 10 flex-body modes

◇ Number of States

- 16 modes estimated x 2 states/mode = 32 states
 - 6 RMS joint-motors x 2 states/actuator = 12 states
- TOTAL = 44 states

◇ Number of Actuators

- RMS joint-motors = 6 actuators
- TOTAL = 6 actuators

◇ Number of Sensors

- 6 modal sensors each plane x 2 planes = 12 sensors
 - 6 RMS joint-motors x 2 sensors/motor (encoder and tachometer) = 12 sensors
 - SPAS sensors: 3 linear accelerometers + 3 rate gyros = 6 sensors
- TOTAL = 30 sensors

◇ Number of Arithmetic Floating-Point Operations (AFLO) Per Sample Data Cycle in state estimator algorithm

The number of multiples in one pass thru the state estimator is

$$\begin{aligned} & \text{states (states + actuators + sensors)} \\ & = 44 (44 + 6 + 30) = 3,520 \text{ Multiplies} \end{aligned}$$

Assuming that there is roughly one add (element accumulate) associated with each multiply for large matrices:

$$\implies 3,520 \times 2 = 7040 \text{ AFLO Per Cycle Thru Algorithm}$$

◇ Cycle Allocation

<u>Algorithm/Operation</u>	<u>Fraction of State Estimator Cycle Time</u>		
	CASE 1	CASE 2	CASE 3
1- State Estimator	1.0	1.0	1.0
2- Controller + Filters	1.0	1.0	1.0
3- Input/Output	1.0	1.0	1.0
4- Sinewave Excitation	0.2	----	----
5- Broadband Excitation	----	1.0	1.0
6- Performance Monitoring Limit Sensing	0.1	----	----
7- Performance Monitoring - Advanced	----	1.0	----
8- Performance Monitoring - System ID	----	----	10.0
Total Cycle Factor	3.3	5.0	14.0

◇ Estimated Computer Speed

- State estimator computations must be completed in sample data cycle time per cycle factor
- Assume sample data rate of 12.5 Hz to be compatible with Orbiter GPC, i.e. sample data cycle time = $1/12.5 = 0.08$ sec
- Speed estimates: (AFLO Per Cycle x Sample Data Rate x Cycle Factor)

$$\text{CASE 1 : } 7040 \times 12.5 \times 3.3 = 290\text{k AFLOPS}$$

$$\text{CASE 2 : } 7040 \times 12.5 \times 5.0 = 440\text{k AFLOPS}$$

$$\text{CASE 3 : } 7040 \times 12.5 \times 14.0 = 1.2\text{M AFLOPS}$$

Appendix D: Orbiter/Carrier Data Rate Estimate

INPUT: Orbiter to Cargo Bay Carrier

	words/cycle
SPAS linear accelerometers	3
SPAS rate gyros	3
RMS joint tachometers	6
RMS joint encoders	6
RMS strain gauges (if DDT&E arm)	6
Modal sensors (to experiment computers)	12
Housekeeping	4
Experiment control commands (from ground and crew)	4
 TOTAL	 = 44 words/cycle

$$44 \text{ words/cycle} \times 12.5 \text{ cycles/sec} \times 16 \text{ bit/word}$$

$$= 8.8 \text{ kbps} \implies 12 \text{ kbps with contingency for growth}$$

OUTPUT: Carrier to Orbiter

	words/cycle
RMS joint-motor commands	6
Status discretes	1
Housekeeping	4
Estimator states	12
Modal sensor data	12
 TOTAL	 = 35 words/cycle

$$35 \text{ words/cycle} \times 12.5 \text{ cycles/sec} \times 16 \text{ bit/word}$$

$$= 7 \text{ kbps} \implies 10 \text{ kbps with contingency for growth}$$

Appendix E: Growing Oscillation Mode of Failure

The growing oscillation mode of failure was simulated using the DRS with the RMS/SPAS system initialized in configuration B (refer to Table 4.3). The RMS Shoulder Pitch (SHP) joint was excited with a sinusoidal rate command using a modified version of the DRS, FXPT. The driving frequency of this sinusoid, $f = 0.09$ Hz, was selected from a prior simulation of a nominal SHP command to the RMS/SPAS system in the same configuration. This frequency corresponds to the dominant first mode of the RMS/SPAS system. The amplitude of this sinusoid servo rate command was selected to produce SHP joint rate limits below the limit specified by the Level-C data for the SPAS payload (< 0.7196 °/sec).

The details of the simulation results are discussed following a brief description of the RMS servo joint control loop.

E.1 Servo Joint Control Loop

Each joint in the RMS contains a servo control loop. The functional organization of this control system is illustrated in Figure E.1. Control algorithms in the RMS software convert input drive commands into an output rate demand resolved for each joint of the arm. This rate demand is output within limits defined according to arm and individual joint loading conditions present at the time of computation. The control algorithms supply this rate command via the MCIU to the control loop input. This input is compared to the actual joint speed supplied by the digital tachometer feedback at the S1 summing junction. The comparison results in an error signal which is sent through a Digital to Analog Converter (DAC) and a filter and passed to a second summing junction, S2. An integral trim function integrates the error signal to overcome friction effects under steady state conditions plus bias effects. At S2, the analog feedback signal is used to control high acceleration demands present in the error signal. After passing through the servo control loop, the error signal is transmitted as an analog rate demand to the motor drive amplifier. This results in an increase in the magnitude of the voltage supplied to the joint motor, and thus a joint drive. [5]

E.2 Simulation Results

The results indicate that the RMS/SPAS was successfully excited at a resonant frequency of 0.09 Hz. This is illustrated in the plot of the SHP servo motor torque (see Figure E.2). During the first 5 seconds of the simulation the SHP joint is driven as commanded but then because it is at resonance (i.e. energy is being pumped into the arm) it doesn't take as much torque as anticipated to swing the arm in the opposite direction. As shown in the servo motor torque plot, the servo overshoots the required torque then backdrives the arm. The limiting that is seen is due

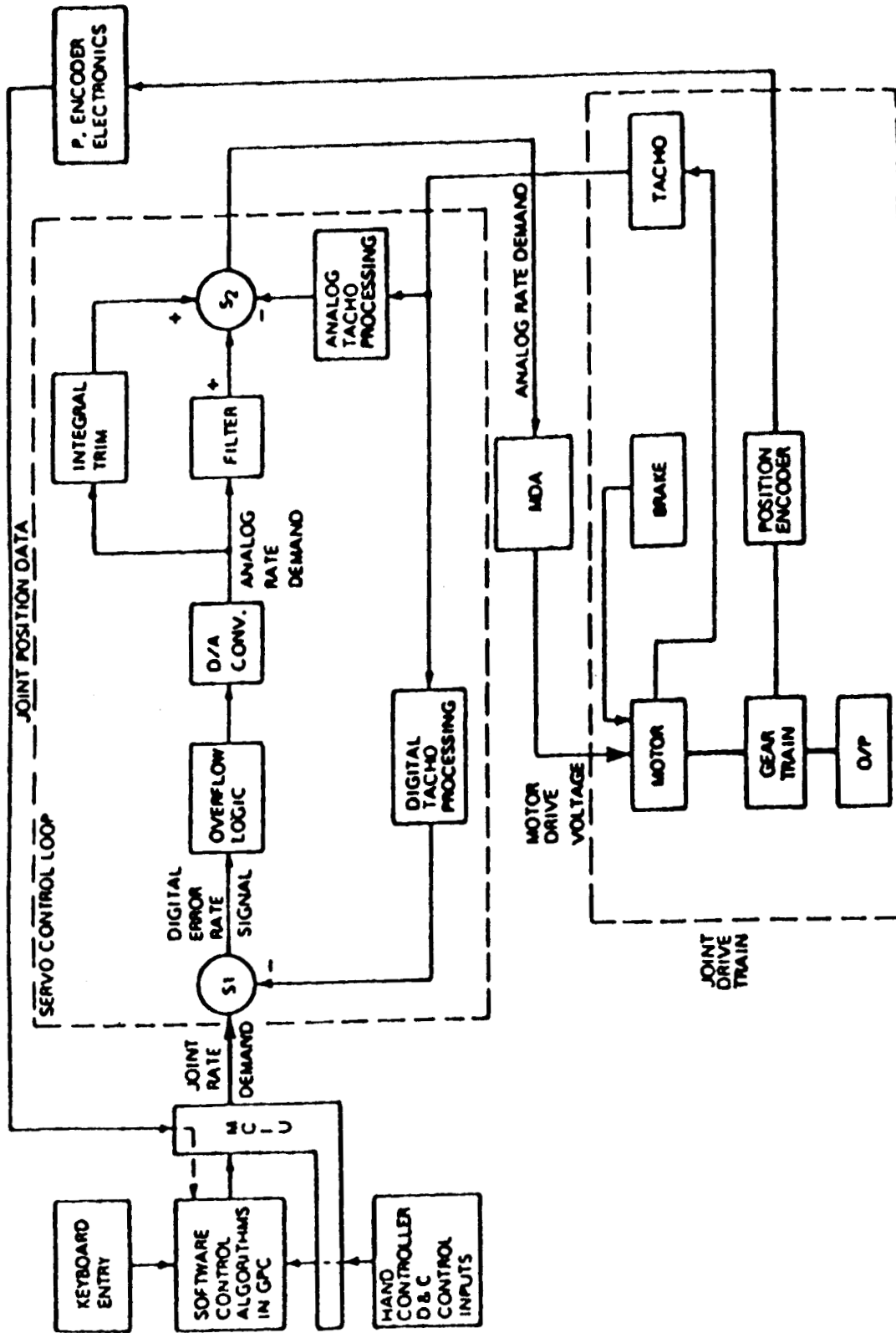


Figure E.1: Control System Block Diagram [5]

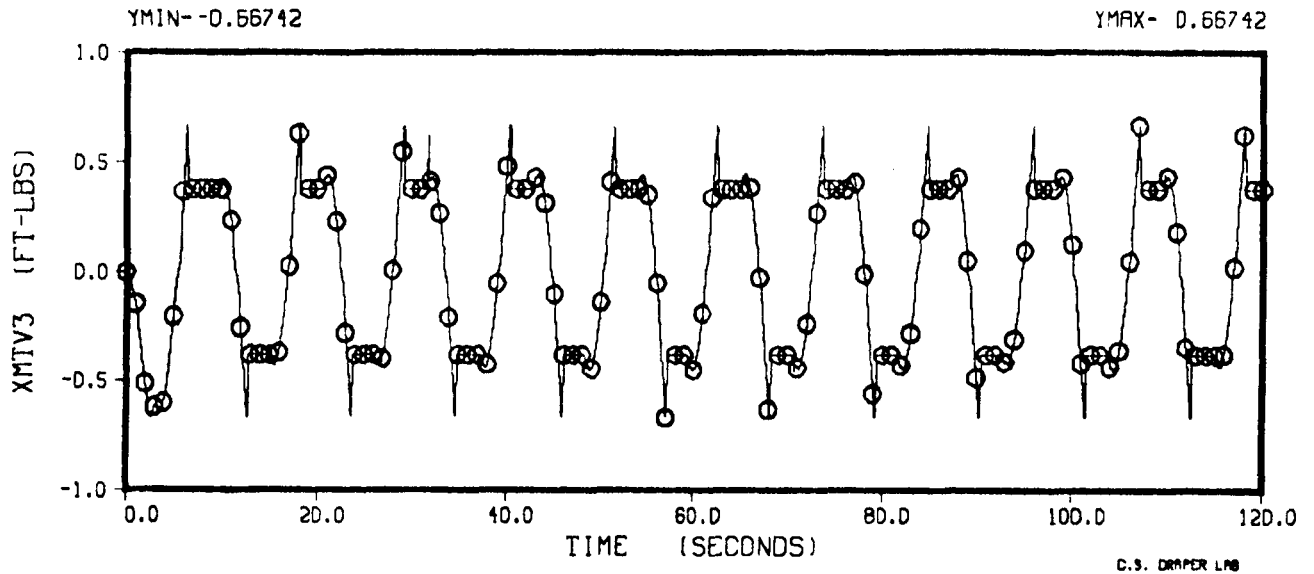


Figure E.2: Shoulder Pitch Servo Motor Torque

to the Backdrive Motor Current Limit which for the SHP joint is

$$(2.57 \text{ amps})(0.17 \text{ ft.-lb. / amp}) = 0.4369 \text{ ft.-lb.}$$

The overshoot that is experienced is due the gearbox efficiency (which quantifies friction losses in the gearbox) transition from forward drive to backward drive. The arm is in forward drive when the motor is driving the joint in the command direction and it is in a backward drive condition when the joint motor is being driven by the load in the reverse of the command direction.

Although the arm is being driven at resonance, the results do not depict any growing oscillatory motion. This is true for the case described above in which the arm is being driven to the backdrive limit and in the linear case when the servo motor torque is below the forward and backdrive current limits. The reason for this is the rate feedback of the servo control loop shown in Figure E.1. This feedback control system maintains the prescribed relationship between the output and the joint rate demand input by comparing these and using the difference as a means of control. In other words, any energy that is pumped in by the resonating oscillation is taken out by the servo.

Assuming that the RMS/CSI experiment will be modifying the software control algorithms in the GPC (refer to Figure E.1) and will not be bypassing the joint housed servo control loops, the arm will be protected from being driven in a growing oscillatory manner. Further, even if the control algorithms demand a joint rate which causes the arm to limit, the arm will not be overloaded. This is illustrated in the plot of the SHP Servo Output Torque, Figure E.3. The output torque is on the order of 1000 ft.-lb. which is less than 70% of the RMS Load Limit for the SHP Drive Axis of 1450 ft.-lb. (see Table E.1).

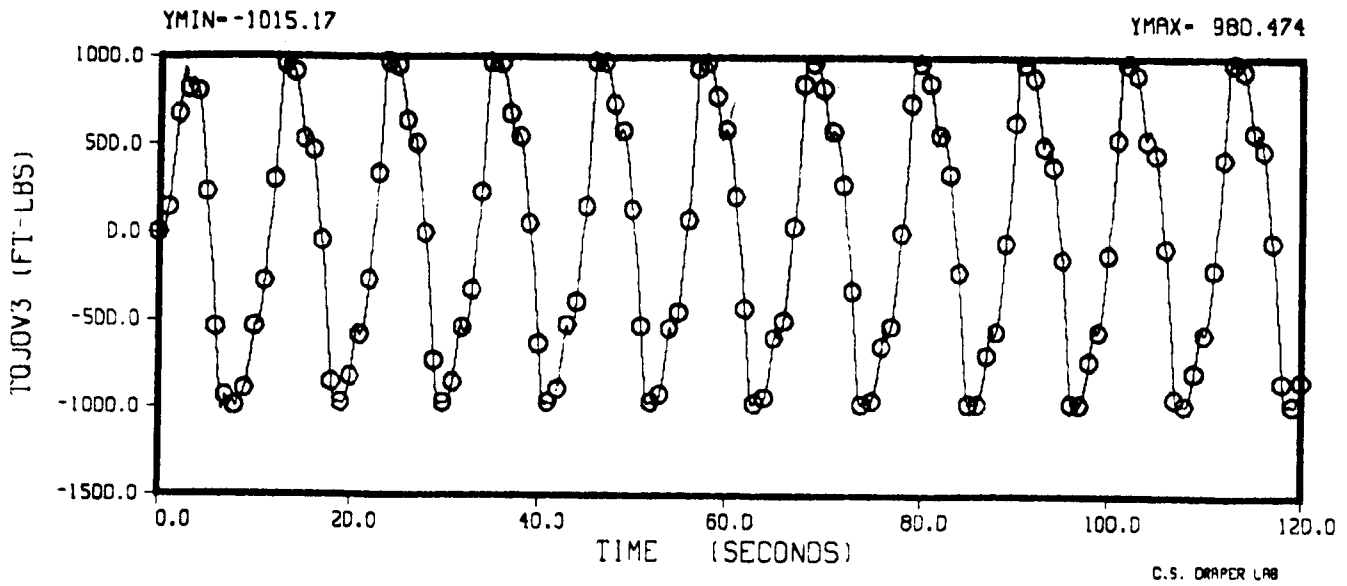


Figure E.3: Shoulder Pitch Servo Output Torque

	SHY	SHP	ELP	WRP	WRY	WRR
MX (ft.-lb.)	2050	1750	550	850	480	480*
MY (ft.-lb.)	1450	1450*	1050*	480*	850	720
MZ (ft.-lb.)	1450*	2280	1800	500	480*	840

* = Drive Axis

Table E.1: RMS Load Limits (for Flight Planning)
(Derived from SPAR SG.409)

**Appendix F:
Experiment Subschedules**

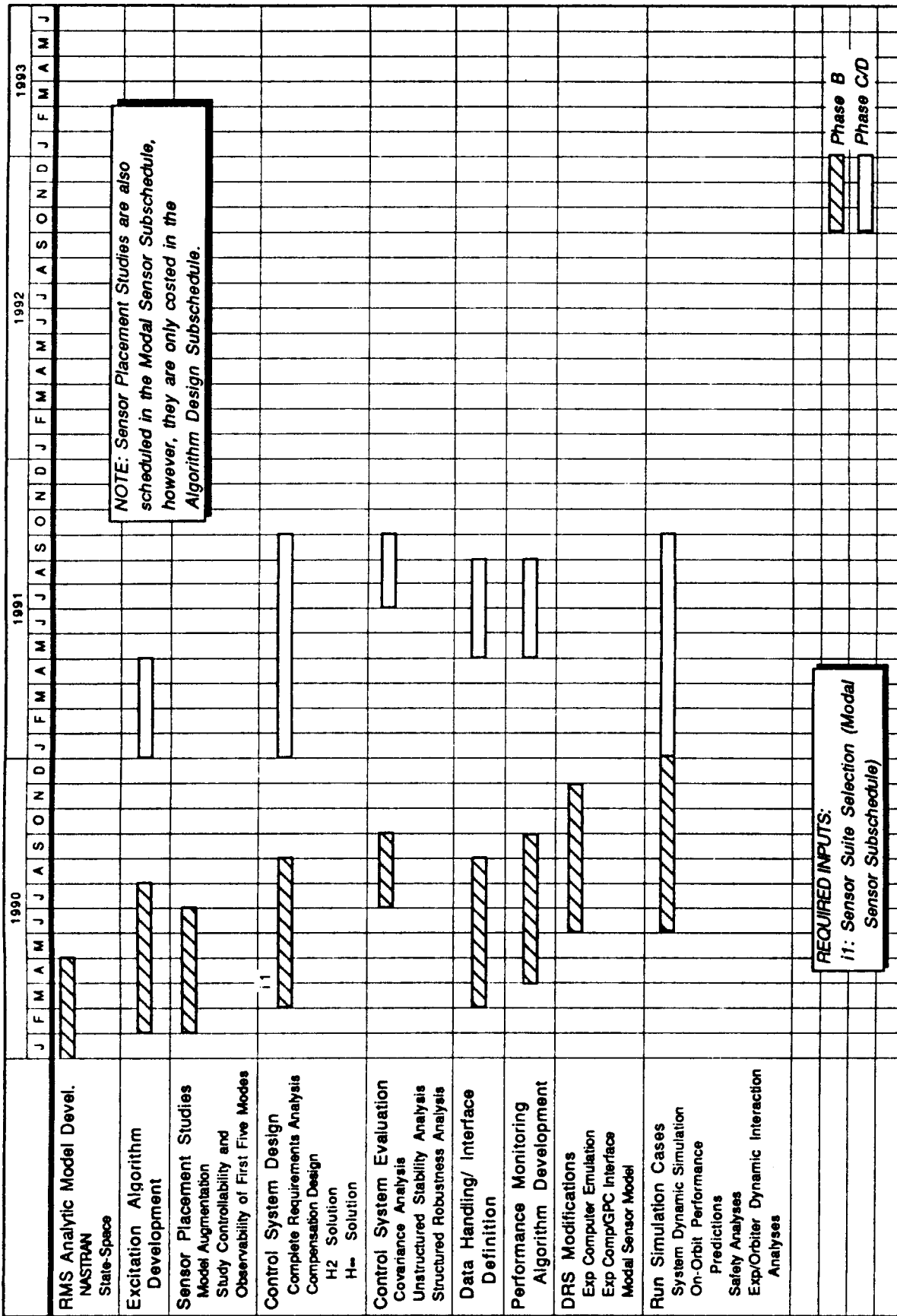


Figure F.1: Algorithm Design Subschedule

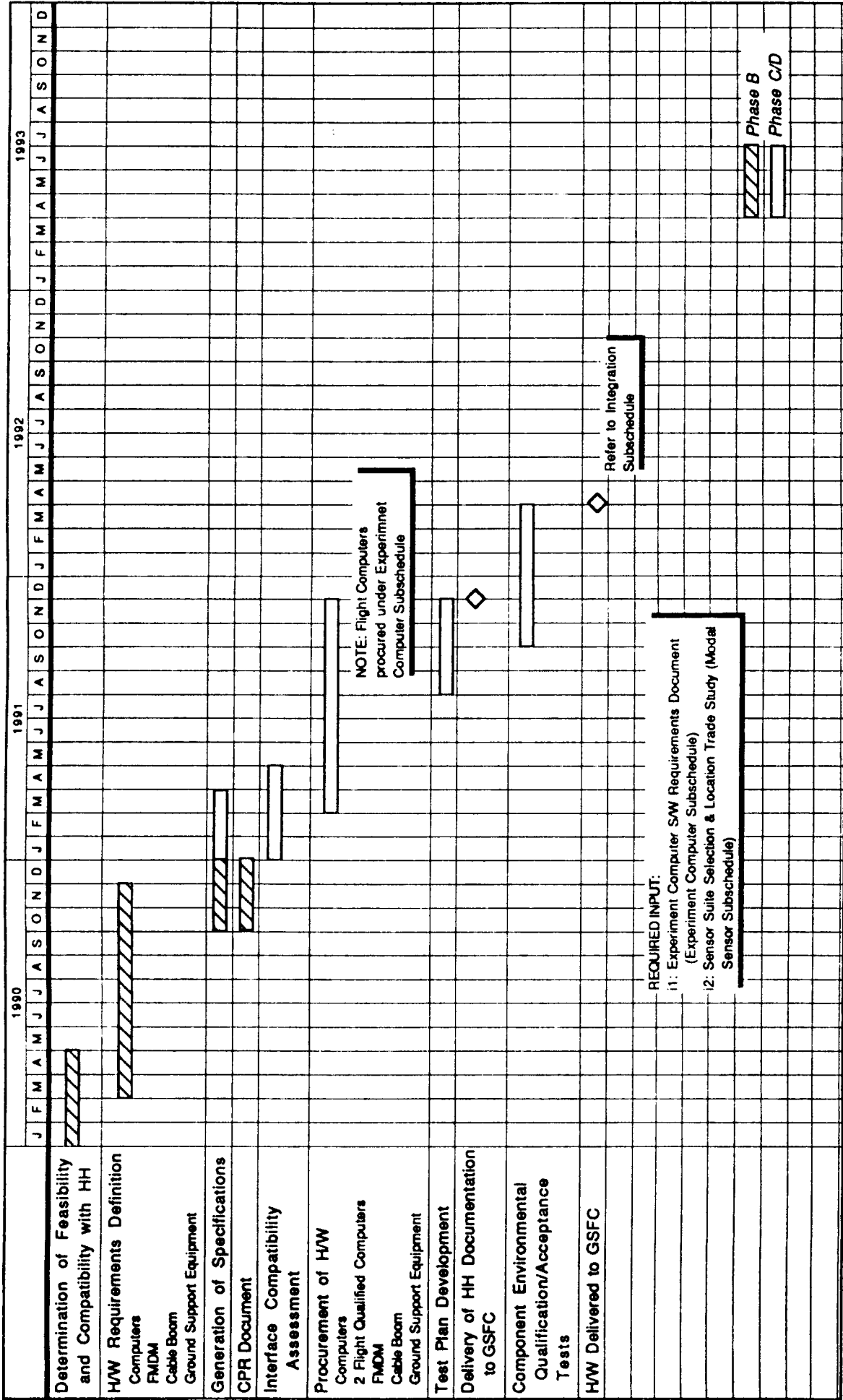


Figure F.3: Hirschhiker Subschedule

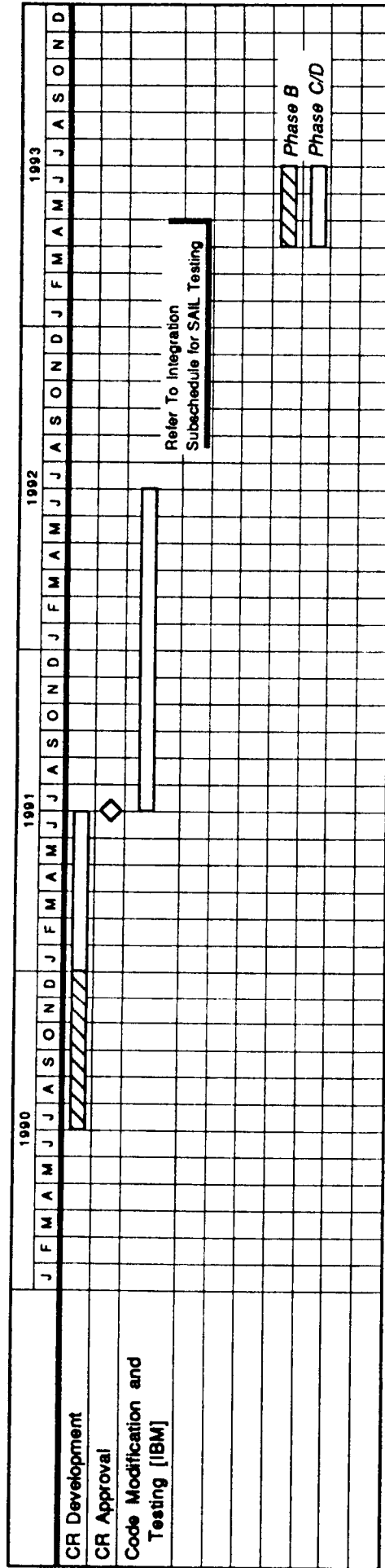


Figure F.4: GPC Software Modification Subschedule

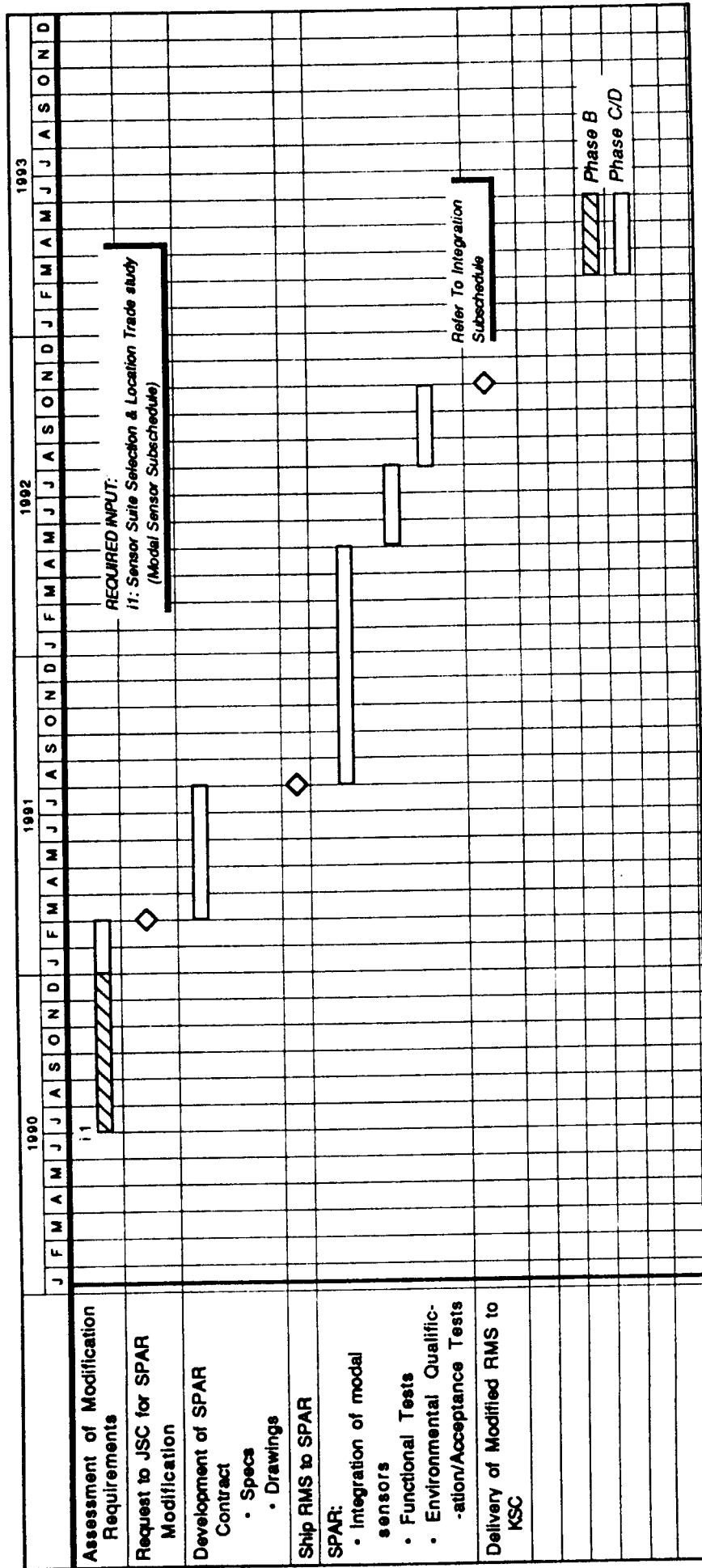


Figure F.5: RMS Modification Subschedule

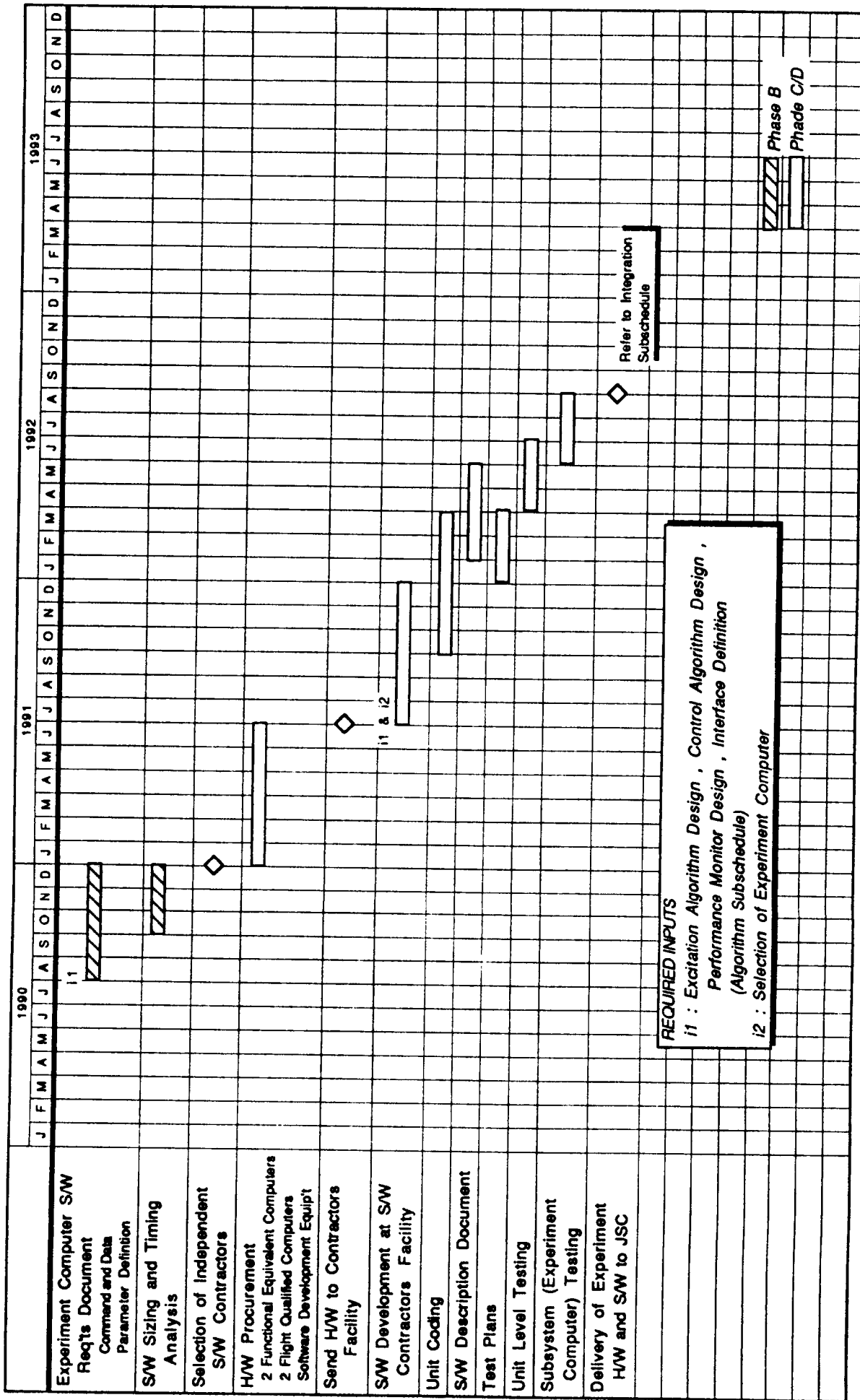


Figure F.6: Experiment Computer Subschedule

Appendix G: Tasks for Phase B Definition Study

The following list of tasks are deferred to the Phase B Definition Study of the RMS-Based CSI Flight Experiment. Design of the flexible body controller, design of the performance monitoring algorithms, and development of specifications for formal quotes were purposely excluded from the scope of the Phase A Feasibility Study. Other listed items surfaced during the Phase A study but funding limitations prevented complete analyses.

- 1) Design the flexible body controller and test on a nonlinear simulation of the RMS to establish feasibility and quantify performance. Also, establish feasibility of a reduced order flexible body controller which resides in the Orbiter GPC and quantify performance.
- 2) Include transport delays of the Shuttle data handling system in the simulation and reevaluate the controller performance and establish the need for an FMDM vs. a MRM on the Hitchhiker.
- 3) Formulate performance monitoring algorithm for experiment computers and define sensor redundancy for two fault tolerance.
- 4) Identify RMS/SPAS configurations which produce closely spaced and dynamically coupled modes.
- 5) Assess excitability/controllability of RMS/SPAS modes from RMS joint motor locations.
- 6) Analyze RMS/SPAS actual flight data from STS 7 for presence of 17 Hz Ku-Band antenna dither disturbance on SPAS accelerometers and gyros and estimate signal to noise ratio.
- 7) Define interface between RMS fastened accelerometers and Hitchhiker mounted experiment computers, i.e. cable boom vs. Shuttle Standard Mixed Cargo Harness (SMCH).
- 8) Develop specifications for installation, functional checkout, and flight qualification of modal sensors on RMS and obtain formal cost quote from SPAR through JSC.
- 9) Develop specifications for modification of GPC software and obtain a formal quote from IBM through JSC for modification and flight validation.
- 10) Negotiate with GSFC for integration and functional checkout of a Hitchhiker-G for use in SAIL at JSC. Determine CSI project cost.
- 11) Negotiate SAIL modifications with JSC to integrate a Hitchhiker-G, model RMS additional sensors and SPAS sensors, and simulate interfaces. Determine CSI project cost.



Report Documentation Page

1. Report No. NASA CR-181952		2. Government Accession No.		3. Recipient's Catalog No.	
4. Title and Subtitle Remote Manipulator System (RMS)-Based Controls-Structures Interaction (CSI) Flight Experiment Feasibility Study				5. Report Date January 1990	
				6. Performing Organization Code	
7. Author(s) Martha E. Demeo				8. Performing Organization Report No. CSDL-R-2186	
				10. Work Unit No. 585-01-71-01	
9. Performing Organization Name and Address The Charles Stark Draper Laboratory, Inc. 555 Technology Square Cambridge, Massachusetts 02139				11. Contract or Grant No. NAS9-17560 & NAS9-18147	
				13. Type of Report and Period Covered Contractor Report Final - 10/88 - 7/89	
12. Sponsoring Agency Name and Address National Aeronautics and Space Administration Langley Research Center Hampton, VA 23665-5225				14. Sponsoring Agency Code	
				15. Supplementary Notes Technical Monitors: Anthony Fontana, Langley Research Center, Hampton, Virginia. Elizabeth Bains, Johnson Space Center, Houston, Texas.	
16. Abstract <p>The objective of this study was to investigate the feasibility of an experiment which will provide an on-orbit validation of Controls-Structures Interaction (CSI) technology. The experiment will demonstrate the on-orbit characterization and flexible-body control of large flexible structure dynamics using the shuttle Remote Manipulator System (RMS) with an attached payload as a test article. By utilizing existing hardware as well as established integration, operation and safety algorithms, techniques, and procedures, the experiment will minimize the costs and risks of implementing a flight experiment. The experiment will also offer spin-off enhancement to both the Shuttle RMS (SRMS) and the Space Station RMS (SSRMS).</p>					
17. Key Words (Suggested by Author(s)) Controls-Structures Interaction Remote Manipulator System Flexible Structure Vibration Control			18. Distribution Statement unclassified - unlimited subject category 16		
19. Security Classif. (of this report) unclassified		20. Security Classif. (of this page) unclassified		21. No. of pages 84	22. Price A05